Induction of Smectic Layering in Nematic Liquid Crystals Using Immiscible Components. 2. Laterally Attached Side-Chain Liquid-Crystalline Poly(norbornene)s and Their Low-Molar-Mass Analogues with Hydrocarbon/Oligodimethylsiloxane Substituents

Coleen Pugh,[*,†] **Jin-Young Bae,**[†,§] **Jayesh Dharia,**[†] **Jason J. Ge,**[‡] **and Stephen Z. D. Cheng**[‡]

Department of Chemistry, Macromolecular Science and Engineering Center, University of Michigan, Ann Arbor, Michigan 48109-1055, and Department of Polymer Science, University of Akron, Akron, Ohio 44329-3909

Received February 19, 1998

ABSTRACT: In contrast to their hydrocarbon analogues which exhibit only nematic mesophases, poly-{5-[[[2′,5′-bis[(4″-(*n*-(dimethylsiloxyl)alkoxy)benzoyl)oxy]benzyl]oxy]carbonyl]bicyclo[2.2.1]hept-2-ene}s and their low-molar-mass model compounds exhibit smectic C mesophases. Since nematic liquid crystals can be forced into layers by terminating their hydrocarbon substituents not only with fluorocarbon segments but also with *flexible* siloxane segments, this supports the hypothesis that the smectic mesomorphism of amphiphilic molecules containing linear fluorocarbon segments is due primarily to the immiscibility of the hydrocarbon and fluorocarbon segments, rather than to a shape persistence of "mesogenic perfluoroalkyl rods". The 2,5-bis[(4′-(*n*-(oligodimethylsiloxyl)alkoxy)benzoyl)oxy]toluenes mimic both the phases formed by the polymers and the general temperatures of their transitions and are therefore excellent models of the polymers. The 5-{[[2′,5′-bis[(4″-(*n*-(oligodimethylsiloxyl)alkoxy)benzoyl)oxy]benzyl]oxy]carbonyl}bicyclo[2.2.1]hept-2-enes were polymerized by ring-opening metathesis polymerization in THF at room temperature using Mo(CHCMe₂Ph)(N-2,6-*i*Pr₂Ph)(O*t*Bu)₂ as the initiator.

Introduction

We have recently demonstrated that nematic liquid crystals can be forced to order into smectic layers by terminating the mesogen's hydrocarbon substituents with fluorocarbon segments.[1,2] Smectic layering can be induced not only in low-molar-mass liquid crystals (LMMLCs) (Chart 1) but also in side-chain liquid-crystalline polymers (SCLCPs) with laterally attached mesogens (Chart 2). Since aliphatic hydrocarbons and fluorocarbons are highly immiscible, we have attributed this layered organization to microsegregation of the two components of the amphiphilic substituents. The extent of incompatibility of aliphatic hydrocarbon and fluorocarbon liquids is exemplified by their endothermic heats of mixing,[3,4] large increases in volume,[3,5] and large positive deviations[4] from ideal solution behavior.[6] These liquid mixtures are therefore macroscopically phase separated at room temperature. For example, the upper critical solution temperature of mixtures of perfluorobutane and *n*-alkanes is above room temperature when *n* ≥ 7; that of mixtures of perfluoroheptane and *n*-alkanes is above room temperature when *n* ≥ 6.[7] The melting behavior of solid mixtures of aliphatic hydrocarbons and fluorocarbons is also highly nonideal, with the individual pure components preferring to associate only with themselves.[8]

Although we attribute the induction of smectic layering in these liquid crystals to the immiscibility of the two components in the amphiphilic substituents,[1,2]

* To whom correspondence should be addressed.
† University of Michigan.
‡ University of Akron.
§ Current address: Department of Polymer Science and Engineering, Sung Kyun Kwan University, 300 Chunchun-dong, Jangan-gu, Suwon, Kyunggi-do 440-746, Korea.

others attribute the smectic mesomorphism of molecules containing linear fluorocarbon segments to the incorporation of "mesogenic perfluoroalkyl rods".[9] Comparison of the crystalline structures of polyethylene (PE) and poly(tetrafluoroethylene) (PTFE) in Table 1 indeed demonstrates that hydrocarbon−fluorocarbon molecules are not only amphiphilic with oleophilic and oleophobic segments but that they are also structurally anisotropic;[10] both their amphiphilic nature and their structural anisotropy promote melting through a multistep process.[11] The distance between two hydrogens on alternate carbon atoms in the planar zigzag conformation of polyethylene is 2.539 Å.[10,12] This conformation can therefore accommodate two hydrogen atoms, each with a van der Waals radius of 1.2 Å. In contrast, the distance between two fluorine atoms on alternate carbons would be 2.595 Å in the planar zigzag conformation of poly(tetrafluoroethylene),[12] which is not sufficient to accommodate two fluorine atoms with van der Waals radii of 1.35 Å. The backbone of PTFE is therefore forced to adopt a helical conformation with a torsion angle of approximately 16°, resulting in a 13₆ helix at temperatures less than 19 °C[12] and a 15₇ helix at temperatures greater than 19 °C.[13] Therefore, the cross-sectional areas of crystalline polyethylene (19.8 Å²)[14] and poly(tetrafluoroethylene) (25.5 Å²)[15] chains also differ.

However, the helical structure and cylindrical surface of crystalline PTFE does not demonstrate that fluorocarbon segments act as rigid rods. The idea that PTFE forms extended chains with a high resistance to conformational change originated from its unusually high melting point (332 °C)[16] and melt viscosity (∼10¹¹ P).[17] However, several theoretical and experimental studies of perfluoroalkanes and PTFE indicate that they are

Chart 1. Low-Molar-Mass Model Compounds of the SCLCPs in Chart 2; 2,5-Bis[(4′-(*n*-alkoxy)benzoyl)oxy]toluenes with Either *n*-Alkoxy Substituents or *n*-Alkoxy Substituents Terminated with Immiscible Fluorocarbon or Oligodimethylsiloxane Substituents
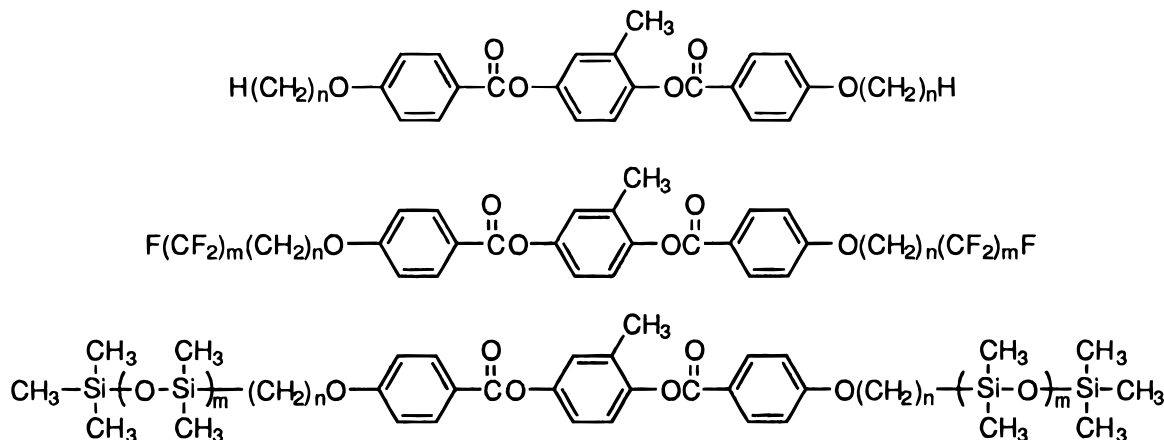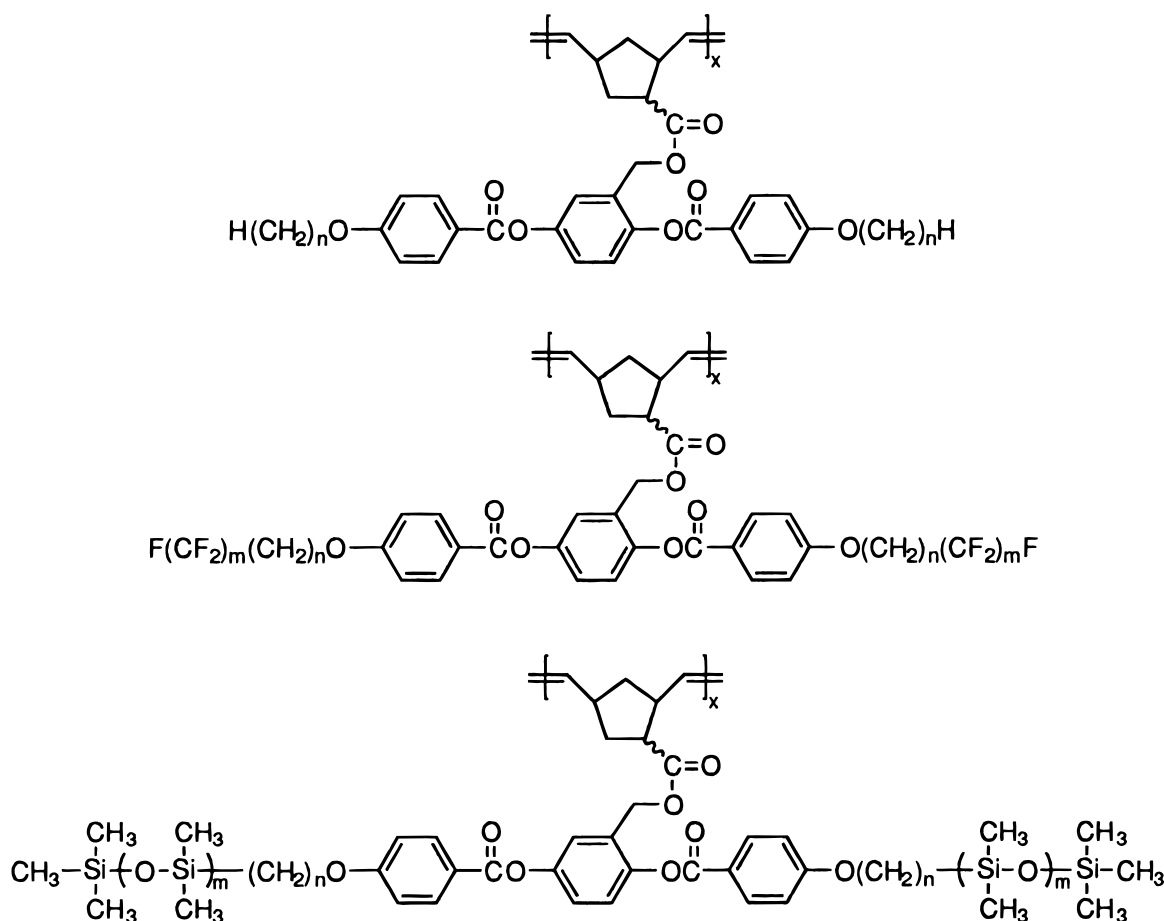
$H(CH_2)_nO$—⬡—CO—⬡(CH_3)—OC—⬡—$O(CH_2)_nH$

$F(CF_2)_m(CH_2)_nO$—⬡—CO—⬡(CH_3)—OC—⬡—$O(CH_2)_n(CF_2)_mF$

CH_3—$Si(O-Si)_m$—$(CH_2)_nO$—⬡—CO—⬡(CH_3)—OC—⬡—$O(CH_2)_n$—$(Si-O)_m Si$—CH_3

Chart 2. Poly(norbornene)s with Laterally Attached 2,5-Bis[(4′-(*n*-alkoxy)benzoyl)oxy]benzyl Mesogens with Either *n*-Alkoxy Substituents, or *n*-Alkoxy Substituents Terminated with Immiscible Fluorocarbon or Oligodimethylsiloxane Substituents
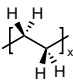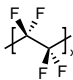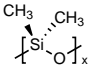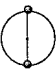
$H(CH_2)_nO$—⬡—CO—⬡—OC—⬡—$O(CH_2)_nH$

$F(CF_2)_m(CH_2)_nO$—⬡—CO—⬡—OC—⬡—$O(CH_2)_n(CF_2)_mF$

CH_3—$Si(O-Si)_m$—$(CH_2)_nO$—⬡—CO—⬡—OC—⬡—$O(CH_2)_n$—$(Si-O)_m Si$—CH_3
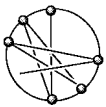
surprisingly flexible. For example, the characteristic ratio[18] of liquid PTFE calculated from improved dipole measurements of *n*-perfluoroalkanes ($C_\infty = 10-15$)[19] and determined experimentally from light-scattering experiments of PTFE ($C_\infty = 8$ at 327 °C)[20] is much smaller than that calculated previously (30 ± 15 at 327 °C),[21] although it is still higher than that of liquid polyethylene ($C_\infty = 6.8$ at 140 °C).[22] The lower characteristic ratios of perfluoroalkanes and PTFE have been accounted for using a six-state rotational isomeric state (RIS) model in which the trans (t) and gauche (g⁺, g⁻) conformations are split into distorted states (t±, g⁺±,

g⁻∓) which further reduce steric crowding by allowing carbon and fluorine atoms to interdigitate; calculated characteristic ratios vary from $C_\infty = 9.8$ at 327 °C to $C_\infty = 15$ at 77 °C.[23] The rotational energy barriers in perfluoroalkanes are therefore smaller than in the corresponding alkanes, yielding a relatively low gauche energy of $E_\sigma = 2.5$ kJ/mol and predicted gauche probabilities varying from 0.22 at 27 °C to 0.36 at 327 °C, vs 0.39 at 27 °C for polyethylene.

    To determine if the smectic mesomorphism exhibited by the fluorinated low-molar-mass model compounds and polymers shown in Charts 1 and 2, respectively, is

Table 1. Comparison of the Conformations of Crystalline Poly(ethylene),[10] Poly(tetrafluoroethylene),[12] and Poly(dimethylsiloxane)[28,29]

	Poly(ethylene)	Poly(tetrafluoroethylene)	Poly(dimethylsiloxane)
van der Waals radii of substituents, Å	1.2	1.35	2.0
distance between substituents on alternate atoms in planar zigzag conformation, Å	2.539	2.595	3.78
spatial representation along the chain			
helix type	1_1 (planar zigzag)	13_6	6_1
torsion angle, deg	0	16	35–40
cross-sectional area, Å^2	19.8	25.5	43

due primarily to the immiscibility of the hydrocarbon and fluorocarbon segments as we have stated,[1,2] or if it is due to the shape persistence of mesogenic perfluoroalkyl rods,[9] we have synthesized the corresponding LMMLCs (Chart 1) and laterally attached SCLCPs (Chart 2) in which the fluorocarbon segments are replaced with immiscible, yet *flexible*, oligodimethylsiloxane segments. That is, it would be impossible for such compounds to exhibit smectic layering based on a shape persistence of the immiscible substituents. For example, poly(dimethylsiloxane) (PDMS) has the lowest glass transition temperature (−127 °C) known for any polymer[16] and a low characteristic ratio ($C_\infty = 6.43$).[24] Neverthelss, Table 1 demonstrates that hydrocarbon–oligodimethylsiloxane molecules are not only amphipilic but that they are also structurally anisotropic. Although PDMS is primarily amorphous, it does exhibit a crystalline melting transition at −40 °C.[25] Due to the alternating bond angles about silicon (∠OSiO 110°) and oxygen (∠SiOSi 143°),[26] crystalline PDMS has a nonrectilinear all-trans conformation which results in an open, ribbonlike 6_1 helix[27,28] and corresponds to a cross-sectional area of 43 Å^2.[29]

Amphiphilic hydrocarbon/oligodimethylsiloxane substituents have also been incorporated into LMMLCs,[30,31] liquid-crystalline dimers,[32–34] and main-chain liquid-crystalline polymers[35–37] (MCLCPs) based on rigid-rod mesogens. With few exceptions,[34,37] these compounds exhibit only smectic mesophases when the oligodimethylsiloxane segment is only a few units long, and many correspond to hydrocarbon analogues that exhibit only nematic mesophases or smectic–nematic phase sequences.[31,33,36] SCLCPs with siloxane spacers[38] or substituents[39] also tend to form smectic mesophases. Nevertheless, the SCLCPs with laterally attached mesogens shown in Chart 2 are the most challenging systems possible for inducing smectic layering; both the molecular architecture[40–42] and the use of only a short spacer[43] disfavor smectic mesomorphism. However, oligodimethylsiloxanes are not nearly as immiscible with hydrocarbons as fluorocarbons are. For example, a 1:1 mixture of *n*-decamethyltetrasiloxane and *n*-hexane requires only 6.2% as much energy to form a homogeneous solution as a 1:1 mixture of *n*-perfluorohexane and *n*-hexane.[44] Therefore, incorporation of immiscible oligodimethylsiloxane segments into the hydrocarbon chemical structure of laterally attached SCLCPs will also test the limits of this immiscibility concept for inducing smectic layering in nematic liquid crystals.

Results and Discussion

Synthesis and Thermotropic Behavior of Model Compounds. The LMMLCs in Chart 1 serve as models of the SCLCPs in Chart 2. They are based on the same mesogen with identical substituents, including a lateral methyl group to mimic the benzylic spacer of the polymers. For example, both the 2,5-bis[(4′-(*n*-alkoxy)benzoyl)oxy]toluenes and the poly{5-[[[2′,5′-bis[(4″-(*n*-alkoxy)benzoyl)oxy]benzyl]oxy]carbonyl]bicyclo[2.2.1]-hept-2-ene}s exhibit only nematic mesophases.[41] The 2,5-bis[(4′-(*n*-(perfluoroalkyl)alkoxy)benzoyl)oxy]toluenes mimic not only the phases (smectic A and smectic C) formed by the poly{5-[[[2′,5′-bis[(4″-(*n*-(perfluoroalkyl)alkoxy)benzoyl)oxy]benzyl]oxy]carbonyl]bicyclo[2.2.1]-hept-2-ene}s but also the general temperatures of their transitions.

The model compounds containing oligodimethylsiloxane segments were synthesized by an analogous route to that used to prepare the model compounds containing fluorocarbon segments. As shown in Scheme 1, ethyl 4-hydroxybenzoate was etherified with an *n*-bromoolefin, followed by saponification of the resulting ethyl 4-(*n*-alkenyloxy)benzoate. The mesogen was then generated by coupling the 4-(*n*-alkenyloxy)benzoic acids with half an equivalent of methylhydroquinone in the presence of dicyclohexylcarbodiimide (DCC) as the dehydrating agent. The oligodimethylsiloxane segments were introduced by platinum-catalyzed hydrosilylation of the double bonds of the *n*-alkenyloxy substituents. We will refer to these model compounds as C*n*Si(*m*+1) according to the number of carbons in the hydrocarbon segments and silicones in the siloxane segments, respectively.

The equilibrium thermal transitions obtained on heating and on cooling the model compounds are summarized in Table 2. The data obtained on heating are from samples that are at thermodynamic equilibrium and generally represent samples crystallized from the melt after annealing at room temperature for several days. As shown by the cooling data in Table 2, crystallization from the melt to the most thermodynamically stable phase is slower than the timescale of the differential scanning calorimetry (DSC) experiment, and the samples either do not crystallize on cooling or crystallize incompletely; only C8Si2 crystallizes in a less stable crystalline phase if it is not annealed. C4Si2, C5Si2, and C4Si3 crystallize after annealing for several days at room temperature but do not crystallize by annealing for 30 min at a temperature slightly lower than the melting point. However, C4Si3 crystallizes extremely slowly and crystallizes only partially after annealing at room temperature for 1−12 months; the

Scheme 1. Synthesis of the 2,5-Bis[(4′-(*n*-(oligodimethylsiloxyl)alkoxy)benzoyl)oxy]toluene Model Compounds (*n* = 4−6, 8; *m* = 1, 2)
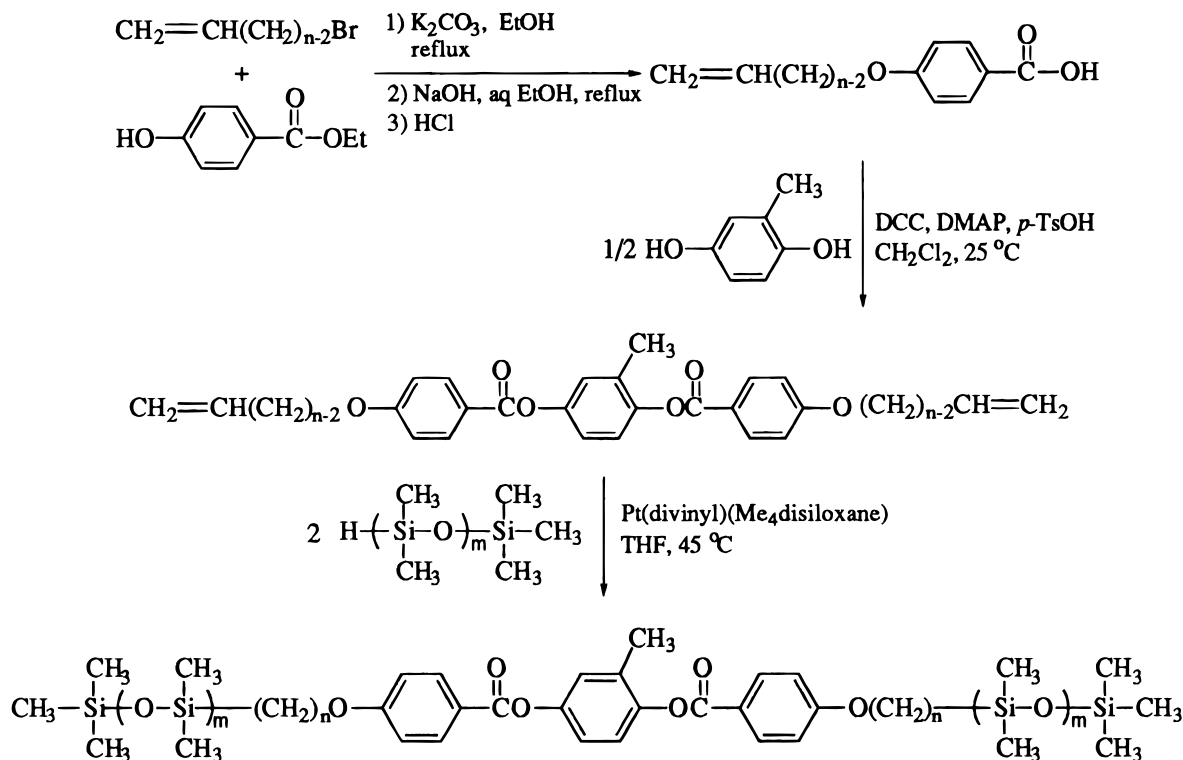
Table 2. Thermal Transitions and Thermodynamic Parameters of 2,5-Bis[(4′-(*n*-(oligodimethylsiloxyl)alkoxy)benzoyl)oxy]toluenes[a]
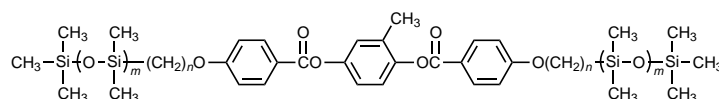
designation	*n*	*m*	phase transitions, °C (Δ*H*, kJ/mol)	
			heating	cooling
C4Si2	4	1	k 52 (29.5) [s$_C$ 42 (6.98)] i	i 34 (6.34) s$_C$
C5Si2	5	1	k 17 (1.70) k 63 (26.3) s$_C$ 70 (7.03) i	i 61 (7.03) s$_C$ 40 (13.6) k 8 (1.64) k
C6Si2	6	1	k 9 (4.26) k 58 (14.5) s$_C$ 74 (9.32) i	i 69 (9.06) s$_C$ 35 (12.1) k −3 (1.63) k
C8Si2	8	1	k 44 (12.1) s$_C$ 88 (9.10) i	i 84 (8.88) s$_C$ 16 (8.56) k
C4Si3	4	2	k 28 (>5.2) [s$_C$ 24 (4.91)] i	i 15 (4.16) s$_C$
C5Si3	5	2	k 66 (33.4) [s$_C$ 54[b]] i	i 38 (3.09) s$_C$ 39 (29.7) k
C6Si3	6	2	s$_C$ 48 (5.88) i	i 43 (4.81) s$_C$
C8Si3	8	2	s$_C$ 71 (5.68) i	i 65 (5.40) s$_C$

[a] k = crystalline; s$_C$ = smectic C; i = isotropic; [monotropic]. [b] Detected only by polarized optical microscopy.

enthalpy of melting of C4Si3 reported in Table 2 is therefore not from a sample that is at thermodynamic equilibrium. The melting points of C6Si3 and C8Si3 are evidently less than −10 °C; they do not crystallize from solution or from the melt, even after annealing at room temperature for 1 year. Only C6Si2 and C5Si3 reach equilibrium during the cooling scan at −10 °C/min. However, crystallization of C5Si3 varies. Although it generally crystallizes at 39 °C, occasionally it crystallizes at 31 °C, thereby revealing the isotropic−smectic C (i−s$_C$) transition. The monotropic s$_C$−i transitions were observed on heating by reheating quenched samples from the s$_C$ mesophase before they crystallized to any extent.

All of the model compounds exhibit only a s$_C$ mesophase, although it tends to be monotropic and observed only on cooling when the hydrocarbon segment is short. Therefore, terminating the *n*-alkoxy substituents with immiscible but flexible oligodimethylsiloxane

segments is also extremely effective at inducing smectic layering in nematic LMMLCs. Both the 2,5-bis[(4′-(*n*-(oligodimethylsiloxyl)alkoxy)benzoyl)oxy]toluenes and the 2,5-bis{[4′-(*n*-(perfluoroalkyl)alkoxy)benzoyl]oxy}-toluenes exhibit smectic mesophases, whereas the 2,5-bis[(4′-(*n*-alkoxy)benzoyl)oxy]toluenes form only nematic mesophases. In contrast to the hydrocarbon−fluorocarbon model compounds whose transition temperatures decrease with increasing hydrocarbon length, all of the transition temperatures of the siloxane analogues increase with increasing hydrocarbon length and decrease with increasing siloxane length. That is, the transition temperatures increase toward the melting point of polyethylene (HDPE mp 138 °C)[16] as the molecule becomes more like polyethylene and decrease toward the melting point of poly(dimethylsiloxane) (−40 °C)[25] as it becomes more like PDMS.

Table 2 also lists the enthalpy changes associated with the phase transitions of the model compounds. The
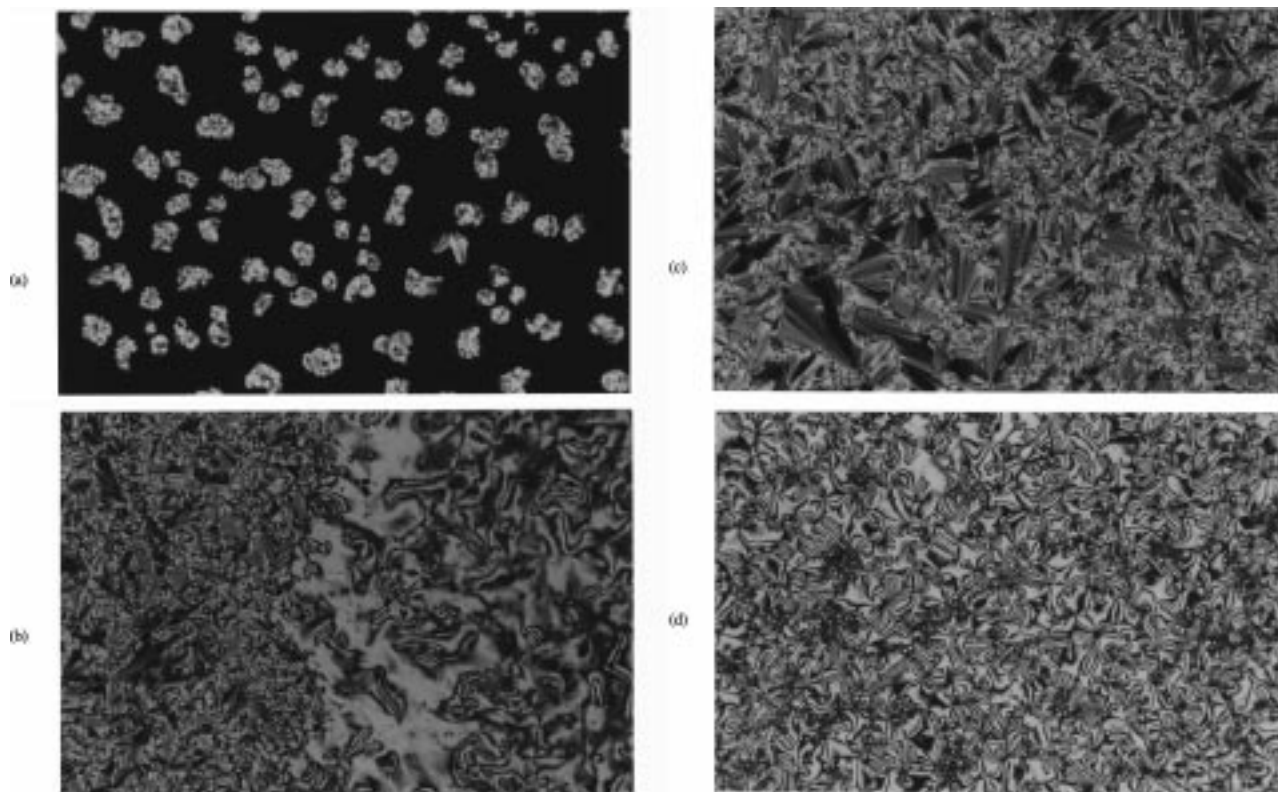
Figure 1. Polarized optical micrographs (200×) observed on cooling 2,5-bis[(4′-(n-(oligodimethylsiloxyl)alkoxy)benzoyl)oxy]toluenes from the isotropic melt: (a) C8Si2, 88.2 °C, s_C irregular droplets and bâtonnets; (b) C8Si2, 85.3 °C, region exhibiting both schlieren and small focal conic fan s_C textures; (c) C8Si2, 85.3 °C, s_C texture with large focal conic fans; (d) C5Si2, 53.5 °C, highly threaded schlieren s_C texture.

change in enthalpy of isotropization is essentially constant as a function of the hydrocarbon length for the heptamethyltrisiloxane (CnSi3) series. However, the change in enthalpy of isotropization of the pentamethyldisiloxane (CnSi2) series increases with increasing hydrocarbon length and is also significantly larger than that of the CnSi3 series; the enthalpy of melting decreases with increasing hydrocarbon length. This indicates that the amphiphilic substituents of the CnSi2 series with the shorter siloxane segments may not be microphase separated.

As shown by the representative polarized optical micrograph in Figure 1a, the s_C texture initially develops in the form of small bâtonnets and irregularly shaped droplets, which are distinctly different from the true droplets formed by a nematic mesophase. These compounds exhibit the two natural textures of the s_C mesophase,[45] often in the same sample preparation (Figure 1b). Compared to the focal conic fan texture of a s_A mesophase, the fans are not sharply defined, even in regions where they are very large (Figure 1c). As shown in Figure 1d, the schlieren texture tends to be highly threaded.

Synthesis and Thermotropic Behavior of the Monomers. Although the model compounds were synthesized by an analogous route to that used to prepare the hydrocarbon−fluorocarbon model compounds, the siloxane-containing monomers could not be synthesized directly from the model compounds by free-radical bromination at the benzylic position. The siloxane segments are extremely sensitive to bromine, acid, base, and many other reagents. For example, bromination of the model compounds using either bromine or N-bromosuccinimide cleaved a substantial

amount of the siloxane segments to regenerate alkenyloxy substituents. We finally synthesized the monomers by the route shown in Scheme 2 by first protecting the carboxylic acid of the 4-(n-alkenyloxy)benzoic acids with a benzyl group, followed by hydrosilylation, and then deprotection of the benzyl group using hydrogen in the presence of palladium on carbon. The amphipilic benzoic acids were then coupled with half an equivalent of 2,5-dihydroxybenzaldehyde using DCC as a dehydrating agent. The key step in the synthesis is the reduction of the aldehyde group using sodium borohydride in the presence of acetic acid. In the absence of acetic acid, reduction of a 2,5-bis[(alkoxybenzoyl)oxy]-benzaldehyde generates a phenol by intramolecular transesterification of the desired benzylalkoxide via a six-membered endo−trig cyclic transition state.[41]
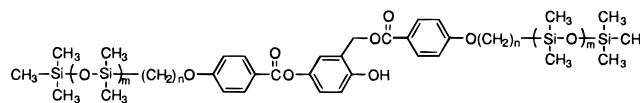
The resulting benzyl alcohol also rearranges readily, and the monomer was therefore synthesized by slowly adding bicyclo[2.2.1]hept-2-ene-5-carboxyl chloride and triethylamine simultaneously but separately to a cold solution of the benzyl alcohol in order to avoid transesterification catalyzed by unreacted acid or base. The resulting monomers are soluble in both polar solvents such as ethanol and nonpolar solvents such as hexane; their solubility in hexane increases as the length of the hydrocarbon segments increases. We will refer to these monomers as mCnSi(m+1) according to the number of carbons in the hydrocarbon segments and silicones in the siloxane segments, respectively.

**Scheme 2. Synthesis of the
5-{[[2′,5′-Bis[(4″-(n-(oligodimethylsiloxyl)alkoxy)benzoyl)oxy]benzyl]oxy]carbonyl}bicyclo[2.2.1]hept-2-ene
(n = 4−6, 8; m = 1, 2) Monomers**

$CH_2=CH(CH_2)_{n-2}O$—〈benzene〉—$\overset{O}{\overset{\|}{C}}$—OH

1) PhCH₂OH, DCC, DMAP, *p*-TsOH
   CH₂Cl₂, 25 °C
2) H-(SiMe₂O)ₘSiMe₃
   Pt(divinyl)(Me₄disiloxane)
   THF, 45 °C
3) H₂, Pd/C, THF, 25 °C

$CH_3-Si(O-Si)_m-(CH_2)_nO$—〈benzene〉—$\overset{O}{\overset{\|}{C}}$—OH

1/2 HO—〈benzene, CHO〉—OH | DCC, DMAP, *p*-TsOH
                          CH₂Cl₂, 25 °C

$CH_3-Si(O-Si)_m-(CH_2)_nO$—〈benzene〉—CO—O—〈benzene, CHO〉—O—C—〈benzene〉—$O(CH_2)_n-(Si-O)_m-Si-CH_3$

NaBH₄, CH₃CO₂H
THF, 25 °C

$CH_3-Si(O-Si)_m-(CH_2)_nO$—〈benzene〉—CO—O—〈benzene, CH₂OH〉—O—C—〈benzene〉—$O(CH_2)_n-(Si-O)_m-Si-CH_3$

〈norbornene〉COCl , NEt₃, CH₂Cl₂
25 °C

$CH_3-Si(O-Si)_m-(CH_2)_nO$—〈benzene〉—CO—O—〈benzene, CH₂-O-C(=O)-norbornene〉—O—C—〈benzene〉—$O(CH_2)_n-(Si-O)_m-Si-CH_3$
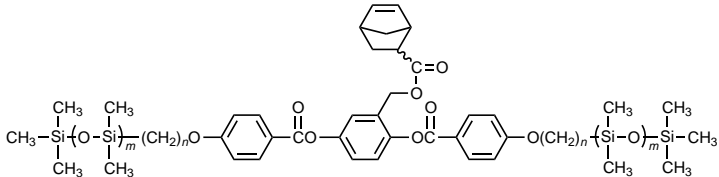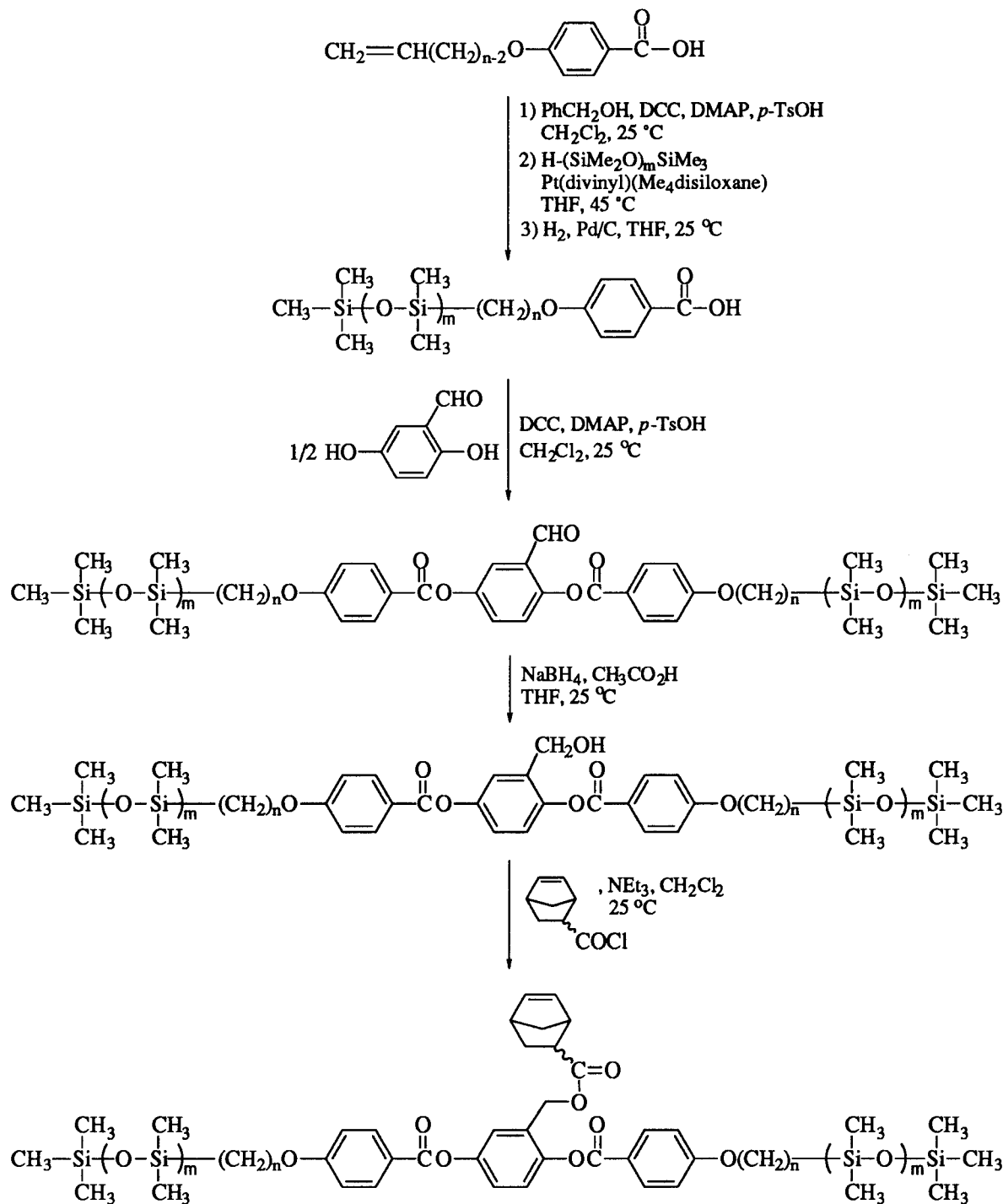
Table 3 summarizes the equilibrium thermal transitions oberved on heating and on cooling the monomers. With the exception of mC8Si2 and mC8Si3, all of the monomers are gummy liquids or waxy solids. Their melting transitions are close to room temperature and are depressed relative to the melting temperatures of the corresponding model compounds. Most of the monomers crystallize from the melt to the most thermodynamically stable phase during the timescale of the DSC experiment. For example, mC8Si2, mC5Si3, mC6Si3, and mC8Si3 reach equilibrium during the cooling scan at −10 °C/min; mC4Si2 recrystallizes partially on cooling and partially on reheating. mC5Si2

and mC6Si2 crystallize in a less stable phase if they are not annealed at room temperature for several days. Only the monomers with the shortest hydrocarbon segments exhibit a s$_C$ mesophase. mC4Si3 apparently does not crystallize from either the melt or from solution and exhibits an enantiotropic s$_C$ mesophase. The s$_C$ mesophase of mC4Si2 is monotropic and observed only on cooling. Therefore, introduction of a large bulky norbornene substituent depresses isotropization of the 2,5-bis[(4′-(n-(oligodimethylsiloxyl)alkoxy)benzoyl)oxy]-toluenes more than melting, as is typical of norbornene monomers containing a laterally attached mesogen.[1,41,42]
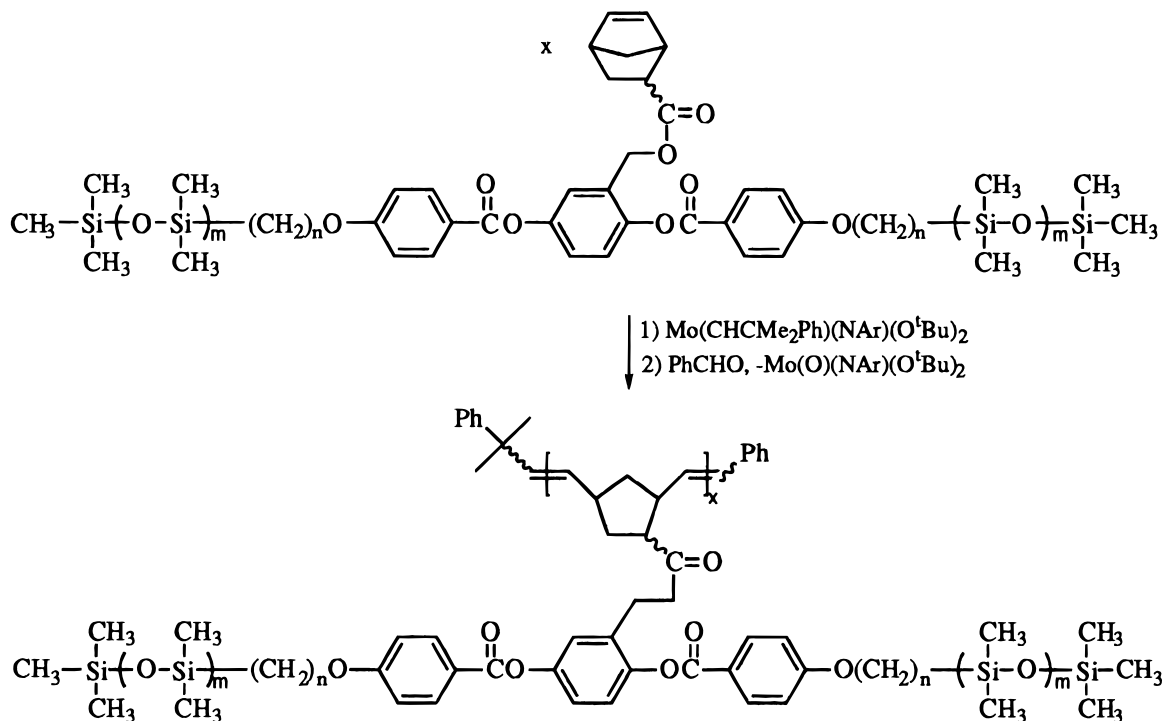
**Table 3. Thermal Transitions and Thermodynamic Parameters of
5-{[[2′,5′-Bis[(4″-(n-(oligodimethylsiloxyl)alkoxy)benzoyl)oxy]benzyl]oxy]carbonyl}bicyclo[2.2.1]hept-2-enes[a]**

			phase transitions, °C (ΔH, kJ/mol)			
designation	n	m	heating		cooling	
mC4Si2	4	1	k 21 (13.1) [s$_C$[b]]	i	i −19 (7.07) s$_C$	
mC5Si2	5	1	k 37 (15.9)	i	i	9 (14.5) k
mC6Si2	6	1	k 50 (24.0)	i	i	27 (21.6) k
mC8Si2	8	1	k 55 (20.9)	i	i	41 (19.8) k
mC4Si3	4	2	s$_C$ −3 (5.95) i		i −14 (6.03) s$_C$	
mC5Si3	5	2	k 6 (4.80) k 17 (11.2)	i	i	6 (16.6) k
mC6Si3	6	2	k 40 (21.8)	i	i	19 (18.1) k
mC8Si3	8	2	k 46 (21.7)	i	i	30 (20.0) k

[a] k = crystalline; s$_C$ = smectic C; i = isotropic; [monotropic]. [b] Could not determine temperature of monotropic transition by polarized optical microscopy because not under temperature control.

**Scheme 3. Ring-Opening Metathesis Polymerization of
5-{[[2′,5′-Bis[(4″-(n-(oligodimethylsiloxyl)alkoxy)benzoyl)oxy]benzyl]oxy]carbonyl}bicyclo[2.2.1]hept-2-enes**

Synthesis and Thermotropic Behavior of the Polymers. As shown in Scheme 3, the 5-{[[2′,5′-bis-[(4″-(n-(oligodimethylsiloxyl)alkoxy)benzoyl)oxy]benzyl]-oxy]carbonyl}bicyclo[2.2.1]hept-2-enes were polymerized by ring-opening metathesis polymerization in THF at room temperature using Mo(CHCMe$_2$Ph)(N-2,6-^{i}Pr$_2$Ph)-(O^{t}Bu)$_2$ as the initiator. All of the polymerizations were performed using [M]$_0$/[I]$_0$ ≈ 50 in order for the polymers' thermotropic behavior to be independent of molecular weight (DP$_n$ ≥ 25).[41,43] Although some of the resulting polymers have GPC-determined number-average degrees of polymerization (DP$_n$ = 37−91 relative to polystyrene) that do not correspond to the initial monomer-to-initiator ratio ([M]$_0$/[I]$_0$ = 41−50), all of the polymers contain more than 25 repeating units (Table 4). The polydispersities are also rather broad (pdi = M_w/M_n = 1.26−1.87), albeit monomodal, which indicates

that we were unable to completely dry these gummy monomers. We will refer to these polymers as pCnSi-(m+1) according to the number of carbons in the hydrocarbon segments and silicones in the siloxane segments, respectively.

The thermotropic behavior of the polymers is summarized in Table 5. All of the polymers exhibit a s$_C$ mesophase, and none of the polymers exhibit a nematic mesophase. Therefore, terminating the n-alkoxy substituents with immiscible but flexible oligodimethylsiloxane segments is also very effective at inducing smectic layering in poly(norbornene)s with laterally attached mesogens. However, the temperature range over which the s$_C$ mesophase is observed is narrow for all of the polymers, and isotropization occurs at a temperature very close to the glass transition temperature. Although the polymers are organized in a

**Table 4. Polymerization of
5-{[[2′,5′-Bis[(4′′-(n-(oligodimethylsiloxyl)alkoxy)benzoyl)oxy]benzyl]oxy]carbonyl}bicyclo[2.2.1]hept-2-enes and
Characterization of the Resulting Polymers[a]**

designation	n	m	$[M]_0/[I]_0$	yield, %	theoretical $10^{-4}M_n$	GPC $10^{-4}M_n$	DP_n	pdi
pC4Si2	4	1	48	82	4.69	4.69	52	1.57
pC5Si2	5	1	41	95	3.87	4.24	45	1.51
pC6Si2	6	1	45	99	4.31	5.08	53	1.51
pC8Si2	8	1	49	83	4.94	7.04	69	1.55
pC4Si3	4	2	48	89	5.10	4.12	39	1.37
pC5Si3	5	2	50	99	5.40	3.99	37	1.26
pC6Si3	6	2	50	78	5.01	7.05	63	1.87
pC8Si3	8	2	47	98	5.45	10.6	91	1.65

[a] Polymerized in THF at room temperature for 2 h; number-average molecular weight (M_n), number-average degree of polymerization (DP_n), and polydispersity (pdi = M_w/M_n) determined by gel permeation chromatography (GPC) relative to polystyrene using mean of RI and UV detectors.

**Table 5. Thermal Transitions and Thermodynamic Parameters of
Poly{5-[[[2′,5′-bis[(4′′-n-((dimethylsiloxyl)alkoxy)benzoyl)oxy]benzyl]oxy]carbonyl]bicyclo[2.2.1]hept-2-ene}s[a]**
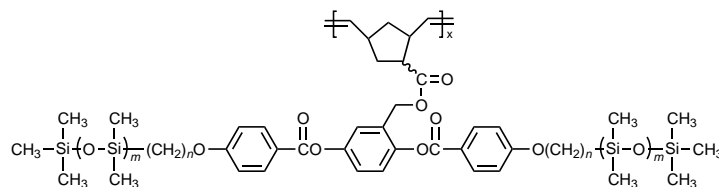
designation	n	m	phase transitions, °C (ΔH, kJ/mol) heating		cooling	
pC4Si2	4	1	g 26	s_C 38 (2.03) i	i	21 g
pC5Si2	5	1	g 48	s_C 57 (4.70) i	i	42 g
pC6Si2	6	1	g 46	s_C 56 (5.55) i	i 50 (0.54) s_C	41 g
pC8Si2	8	1	g 51 k 60 (2.50)	s_C 72 (3.37) i	i 64 (3.00) s_C	53 g
pC4Si3	4	2	g 17	s_C 23 (2.11) i	i	16 g
pC5Si3	5	2	g 44	s_C 54 (4.99) i	i 45 (0.73) s_C	36 g
pC6Si3	6	2	g 46	s_C 55 (4.10) i	i 46 (0.77) s_C	37 g
pC8Si3	8	2	g 50 k 61 (3.94)	s_C 72 (2.47) i	i 65 (3.17) s_C	49 g

[a] g = glass; k = crystalline or unidentified smectic phase; s_C = smectic C; i = isotropic.

smectic mesophase as precipitated from solution, the proximity of isotropization to the glass transition impedes reordering into the s_C mesophase upon cooling from the isotropic melt. Once they are heated through isotropization and cooled to room temperature, most of the polymers require several hours of annealing before they completely reorganize (Figure 2). As shown by the annealed heating scans in Figure 2, pC8Si2 and pC8Si3 also exhibit an additional endotherm due to a transition from a more ordered phase to the s_C mesophase; this more ordered phase evidently forms only from the melt or solid state since it is not exhibited by pC8Si2 and pC8Si3 immediately after precipitating from solution.

We could not confirm the s_C mesophase of these polymers by polarized optical microscopy. They exhibit dark, highly threaded schlieren textures that are not distinctive. However, the s_C mesophase was confirmed by wide-angle X-ray diffraction powder and fiber patterns of the polymers annealed at room temperature overnight, in which the s_C alignment is frozen in the glassy state. As presented in Figure 3, the WAXD patterns of unoriented films exhibit a sharp diffraction at low angles, corresponding to the lamellar thickness, and a diffuse diffraction at wide angles, which demonstrates that the mesogens are disordered within the layer planes. The representative fiber pattern of pC4Si2 shown in Figure 4 demonstrates that the disordered smectic mesophase is a s_C phase. The s_C mesophase is clearly identified by the four low-angle reflections at 2θ = 3° in each quadrant. The tilted layer normal is

approximately 50° from the meridian (fiber) direction. The pair of diffuse scattering at approximately $2\theta = 19°$ on the equator is due to the intermolecular lateral packing. We will report the detailed investigation of the packing of these polymers in the future.

As with the low-molar-mass model compounds, all of the transition temperatures increase with increasing hydrocarbon length as the polymer becomes more like polyethylene and decrease with increasing siloxane length as it becomes more like poly(dimethylsiloxane). Comparison of the data in Tables 2 and 5 demonstrates that both the mesophases and the isotropization temperatures of the model compounds and poly(norbornene)s are nearly identical. The 2,5-bis[(4′-(n-(oligodimethylsiloxyl)alkoxy)benzoyl)oxy]toluenes are therefore excellent models of the poly{5-[[[2′,5′-bis[(4′′-(n-(dimethylsiloxyl)alkoxy)benzoyl)oxy]benzyl]oxy]carbonyl]bicyclo[2.2.1]hept-2-ene}s.

Conclusions

Nematic liquid crystals can be forced to order into smectic layers by terminating their hydrocarbon substituents with immiscible, yet extremely flexible, oligodimethylsiloxane segments. This supports the hypothesis that the smectic mesomorphism of amphiphilic molecules containing linear fluorocarbon segments is due primarily to the immiscibility of the hydrocarbon and fluorocarbon segments, rather than to a shape persistence of mesogenic perfluoroalkyl rods. It is also
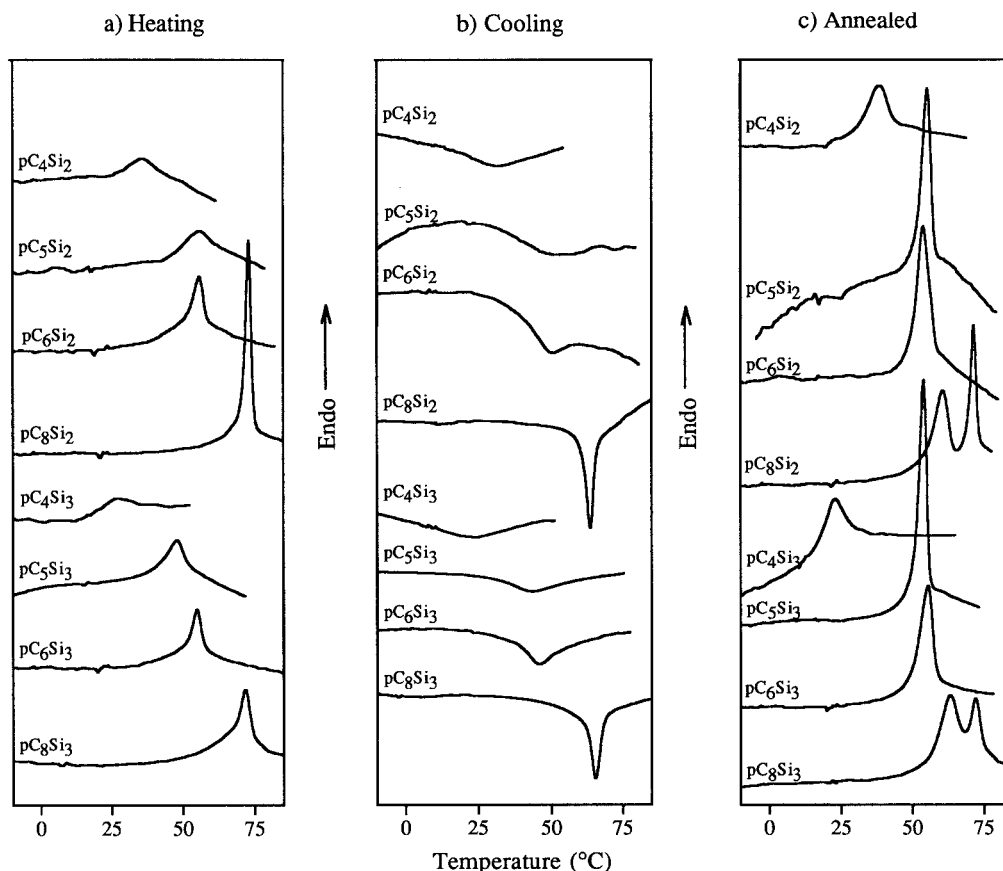
a) Heating   b) Cooling   c) Annealed

Figure 2. Normalized differential scanning calorimetry traces (10 °C/min) of the poly{5-[[[2′,5′-bis[(4″-(*n*-(oligodimethylsiloxyl)-alkoxy)benzoyl)oxy]benzyl]oxy]carbonyl]bicyclo[2.2.1]hept-2-ene}s (*n* = 4–6, 8; *m* = 1, 2) observed on (a) second and subsequent heating scans, (b) cooling scans, and (c) heating scans of samples annealed at room temperature for at least 8 days.
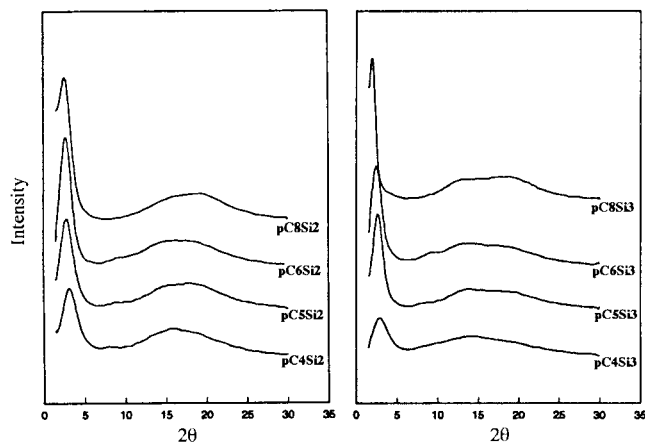

Figure 3. Wide-angle X-ray diffraction patterns of unoriented films of poly{5-[[[2′,5′-bis[(4″-(*n*-(oligodimethylsiloxyl)alkoxy)-benzoyl)oxy]benzyl]oxy]carbonyl]bicyclo[2.2.1]hept-2-ene}s recorded in the glassy state at room temperature.

in spite of the fact that siloxanes are not nearly as immiscible with hydrocarbons as fluorocarbons are.
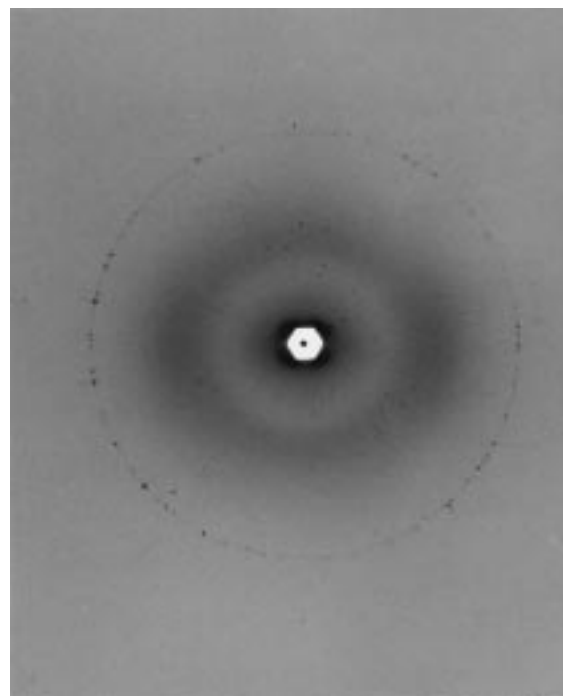
Experimental Section

Figure 4. Wide-angle X-ray diffraction pattern of an oriented fiber of poly{5-[[[2′,5′-bis[(4″-(*n*-(pentamethyldisiloxyl)butoxy)-benzoyl)oxy]benzyl]oxy]carbonyl]bicyclo[2.2.1]hept-2-ene}-(pC4Si2) recorded in the glassy state at room temperature.

oxy)benzoates, 4-(*n*-alkenyloxy)benzoic acids, 2,5-bis[(4′-(*n*-alkenyloxy)benzoyl)oxy]toluenes (*n* = 4−6, 8), and bicyclo-[2.2.1]hept-2-ene-5-carboxyl chloride (73:27 endo:exo) were synthesized as described previously.[1] Benzaldehyde (Aldrich, >99%) was distilled under N_2 before use. Triethylamine was distilled from KOH under N_2 before use. Hexane used in all drybox procedures was washed with 5% HNO_3 in H_2SO_4, stored over $CaCl_2$, and then distilled from purple sodium benzophenone ketyl under N_2. Dry CH_2Cl_2 was obtained by washing with 10% HNO_3 in H_2SO_4, stored over $CaCl_2$, and then distilled from CaH_2 under N_2. Reagent-grade tetrahydrofuran (THF) was dried by distillation from purple sodium benzophenone ketyl under N_2. THF used as a polymerization solvent was vacuum transferred from purple sodium benzophenone ketyl on a high vacuum line and then vigorously degassed by several freeze−pump−thaw cycles immediately before use. All other reagents and solvents were commercially available and were used as received.

Techniques. All polymerizations were performed under a N_2 atmosphere in a Vacuum Atmospheres drybox. All other reactions were performed outside the drybox under a N_2 atmosphere. ^{1}H NMR spectra (δ, ppm) were recorded on either a Bruker AC-200 (200-MHz) or a Bruker AM-300 (300-MHz) spectrometer. Unless noted otherwise, all spectra were recorded in $CDCl_3$ with TMS as an internal standard. Relative molecular weights were determined by gel permeation chromatography (GPC) at 35 °C using THF as the solvent (1.0 mL/min), a set of 50-, 100-, 500-, 10^4-, and linear (50−10^4-Å) Styragel 5 μ columns, a Waters 486 tunable UV/vis detector set at 290 nm, and a Waters 410 differential refractometer.

The thermotropic behavior of all compounds was determined by a combination of differential scanning calorimetry (DSC) and polarized optical microscopy. A Perkin-Elmer DSC-7 differential scanning calorimeter was used to determine the thermal transitions which were read as the maximum or minimum of the endothermic or exothermic peaks, respectively. Glass transition temperatures (T_gs) were read as the middle of the change in heat capacity. All heating and cooling rates were 10 °C/min. Both enthalpy changes and transition temperatures were determined using indium and zinc as calibration standards. A Leitz Laborlux 12 Pol S polarized optical microscope (magnification 200×) equipped with a Mettler FP82 hot stage and a Mettler FP90 central processor was used to observe the thermal transitions and to analyze the anisotropic textures.[45] Thin samples were prepared by melting a minimum amount of compound between a clean glass slide and a cover slip and rubbing the cover slip with a spatula.

Wide-angle X-ray diffraction (WAXD) experiments were carried out on a Rigaku 12-kW rotating-anode generator (Rotaflex RU-200BH) at room temperature (50 kV/250 mA). All of the powder samples were measured in the transmission mode. The Ni-filtered Cu Kα radiation was monochromatized using a graphite crystal. A diffractometer was coupled with the generator, and a scanning 2θ angle range was between 1.5° and 30° at a scanning rate of 3°/min. The background of air scattering for each sample measurement was subtracted using a blank scan. Fiber samples with a diameter of approximately 50 μm were prepared by melt spinning. The as-spun fibers were mounted in a vacuum flat camera which was coupled with a Rigaku tube X-ray generator (40 kV/30 mA). The same Cu Kα radiation was used. Silicon powders with known crystal sizes were used in a 2θ angle calibration (28.46°). The exposure time was 24 h.

Synthesis of the Monomers and Precursors. Benzyl 4-(*n*-Alkenyloxy)benzoates (*n* = 4−6, 8). The benzyl 4-(*n*-alkenyloxy)benzoates were prepared in 76−90% yield as in the following example. A solution of 4-(*n*-but-3′-enyloxy)benzoic acid (4.4 g, 23 mmol), benzyl alcohol (2.4 g, 23 mmol), DCC (5.2 g, 25 mmol), DMAP (2.8 g, 23 mmol), and *p*-toluenesulfonic acid (0.44 g, 2.3 mmol) in dry CH_2Cl_2 (40 mL) was stirred at room temperature for 12 h. The resulting white precipitate was filtered off, and the solvent was removed from the filtrate by rotary evaporation. The residue was purified by column chromatography using silica gel as the stationary phase and

CH_2Cl_2/hexanes (1:1) as the eluant to yield 5.1 g (80%) of benzyl 4-(*n*-but-3′-enyloxy)benzoate as a colorless liquid. ^{1}H NMR: 2.56 (m, CH_2CH$_2$O), 4.06 (t, OCH_2), 5.16 (m, =CH_2), 5.34 (s, OCH_2Ph), 5.90 (m, =CH), 6.91 (d, 2 aromatic H ortho to OCH$_2$), 7.40 (m, 5 aromatic H of benzyl ring), 8.03 (d, 2 aromatic H ortho to CO$_2$).

Benzyl 4-(*n*-Pent-4′-enyloxy)benzoate. ^{1}H NMR: 1.90 (m, CH_2CH$_2$O), 2.25 (q, CH_2CH=), 4.02 (t, OCH_2), 5.05 (m, =CH_2), 5.34 (s, OCH_2Ph), 5.84 (m, =CH), 6.90 (d, 2 aromatic H ortho to OCH$_2$), 7.39 (m, 5 aromatic H of benzyl ring), 8.02 (d, 2 aromatic H ortho to CO$_2$).

Benzyl 4-(*n*-Hex-5′-enyloxy)benzoate. ^{1}H NMR: 1.58 (m, CH_2CH$_2$CH=), 1.82 (m, CH_2CH$_2$O), 2.13 (q, CH_2CH=), 4.01 (t, OCH_2), 5.01 (m, =CH_2), 5.34 (s, OCH_2Ph), 5.85 (m, =CH), 6.90 (d, 2 aromatic H ortho to OCH$_2$), 7.40 (m, 5 aromatic H of benzyl ring), 8.02 (d, 2 aromatic H ortho to CO$_2$).

Benzyl 4-(*n*-Oct-7′-enyloxy)benzoate. ^{1}H NMR: 1.40 (m, [CH_2]$_3$), 1.79 (m, CH_2CH$_2$O) 2.07 (q, CH_2CH=), 4.00 (t, OCH_2), 4.98 (m, =CH_2), 5.34 (s, OCH_2Ph), 5.80 (m, =CH), 6.90 (d, 2 aromatic H ortho to OCH$_2$), 7.40 (m, 5 aromatic H of benzyl ring), 8.02 (d, 2 aromatic H ortho to CO$_2$).

Benzyl 4′-(*n*-(Oligodimethylsiloxyl)alkoxy)benzoates (*n* = 4−6, 8; *m* = 1, 2). Benzyl 4′-(*n*-(oligodimethylsiloxyl)-alkoxy)benzoates were prepared in 77−98% yield. In a typical procedure, a trace amount of platinum divinyltetramethyl-disiloxane was added to a solution of 4-(*n*-but-4′-enyloxy)-benzoate (2.5 g, 8.8 mmol) and pentamethyldisiloxane (1.6 g, 11 mmol) in dry THF (20 mL). After stirring at 45 °C for 24 h, the solvent was removed by rotary evaporation. The residue was purified by column chromatography using silica gel as the stationary phase and CH_2Cl_2/hexanes (1:1) as the eluant to yield 3.2 g (85%) of benzyl 4′-(*n*-(pentamethyldisiloxyl)butoxy)-benzoate as a colorless viscous liquid. The ^{1}H NMR spectra of the benzyl 4′-(*n*-(oligodimethylsiloxyl)butoxy)benzoates with *m* = 1, 2 are identical: 0.08 (s, SiCH_3, 6*m* + 9 H), 0.60 (t, CH_2Si), 1.54 (m, CH_2CH$_2$Si), 1.84 (m, CH_2CH$_2$O), 4.02 (t, OCH_2), 5.35 (s, OCH_2Ph), 6.92 (d, 2 aromatic H ortho to OCH$_2$), 7.43 (m, 5 aromatic H of benzyl ring), 8.03 (d, 2 aromatic H ortho to CO$_2$Ar).

The ^{1}H NMR spectra of the benzyl 4′-(*n*-(oligodimethylsi-loxyl)pentoxy)benzoates with *m* = 1, 2 are identical: 0.06 (s, SiCH_3, 6*m* + 9 H), 0.55 (t, CH_2Si), 1.40 (m, CH_2CH$_2$Si≡), 1.48 (m, CH_2CH$_2$CH$_2$O), 1.82 (m, CH_2CH$_2$O), 4.00 (t, OCH_2), 5.34 (s, OCH_2Ph), 6.90 (d, 2 aromatic H ortho to OCH$_2$), 7.40 (m, 5 aromatic H of benzyl ring), 8.02 (d, 2 aromatic H ortho to CO$_2$-Ar).

The ^{1}H NMR spectra of the benzyl 4′-(*n*-(oligodimethylsi-loxyl)alkoxy)benzoates with *n* = 6, 8 and *m* = 1, 2 are identical: 0.08 (s, SiCH_3, 6*m* + 9 H), 0.53 (t, CH_2Si), 1.35 (m, [CH_2]$_{n−4}$, 2[*n* − 4] H), 1.49 (m, CH_2CH$_2$CH$_2$O), 1.80 (m, CH_2-CH$_2$O), 4.00 (t, OCH_2), 5.34 (s, OCH_2Ph), 6.90 (d, 2 aromatic H ortho to OCH$_2$), 7.40 (m, 5 aromatic H of benzyl ring), 8.02 (d, 2 aromatic H ortho to CO$_2$Ar).

4′-(*n*-(Oligodimethylsiloxyl)alkoxy)benzoic Acids (*n* = 4−6, 8; *m* = 1, 2). The 4′-(*n*-(oligodimethylsiloxyl)alkoxy)-benzoic acids were prepared in 78−95% yield. In a typical procedure, H_2 gas was slowly bubbled through a mixture of benzyl 4′-(*n*-(pentamethyldisiloxyl)butoxy)benzoate (2.3 g, 5.3 mmol) and Pd/C (0.80 g) in THF (25 mL) at room temperature for 12 h. The insoluble material was filtered off, and the filtrate was concentrated in vacuo to yield 1.4 g (78%) of 4′-(*n*-(pentamethyldisiloxyl)butoxy)benzoic acid as a white solid. The 4′-(*n*-(oligodimethylsiloxyl)alkoxy)benzoic acids were used without further purification. The ^{1}H NMR spectra of the 4′-(*n*-(oligodimethylsiloxyl)butoxy)benzoic acids with *m* = 1, 2 are identical: 0.08 (s, SiCH_3, 6*m* + 9 H), 0.60 (t, CH_2Si), 1.53 (m, CH_2CH$_2$Si), 1.84 (m, CH_2CH$_2$O), 4.04 (t, OCH_2), 6.93 (d, 2 aromatic H ortho to OCH$_2$), 8.05 (d, 2 aromatic H ortho to CO$_2$).

The ^{1}H NMR spectra of the 4′-(*n*-(oligodimethylsiloxyl)-pentoxy)benzoic acids with *m* = 1, 2 are identical: 0.08 (s, SiCH_3, 6*m* + 9 H), 0.56 (t, CH_2Si), 1.43 (m, CH_2CH$_2$Si), 1.48 (m, CH_2CH$_2$CH$_2$O), 1.82 (m, CH_2CH$_2$O), 4.02 (t, OCH_2), 6.93 (d, 2 aromatic H ortho to OCH$_2$), 8.05 (d, 2 aromatic H ortho to CO$_2$Ar).

The ^{1}H NMR spectra of the 4′-(*n*-(oligodimethylsiloxyl)-alkoxy)benzoic acids with $n = 6, 8$ and $m = 1, 2$ are identical: 0.06 (s, SiCH_3, $6m + 9$ H), 0.53 (t, CH_2Si), 1.37 (m, [CH_2]$_{n-4}$, 2[$n - 4$] H), 1.47 (m, CH_2CH$_2$CH$_2$O), 1.81 (m, CH_2CH$_2$O), 4.02 (t, OCH_2), 6.93 (d, 2 aromatic H ortho to OCH$_2$), 8.06 (d, 2 aromatic H ortho to CO$_2$Ar).

2,5-Bis[(4′-(*n*-(oligodimethylsiloxyl)alkoxy)benzoyl)-oxy]toluenes ($n = 4$–$6, 8$; $m = 1, 2$). The 2,5-bis[(4′-(*n*-(oligodimethylsiloxyl)alkoxy)benzoyl)oxy]toluenes were prepared in 77–97% yield as in the following example. A trace amount of platinum divinyltetramethyldisiloxane was added to a solution of 2,5-bis[(4′-(*n*-but-3″-enyloxy)benzoyl)oxy]toluene (1.0 g, 2.1 mmol) and pentamethyldisiloxane (0.69 g, 4.7 mmol) in dry THF (7 mL). After stirring at 45 °C for 24 h, the solvent was removed by rotary evaporation. The residue was purified by column chromatography using silica gel as the stationary phase and CH$_2$Cl$_2$ as the eluant to yield 1.4 g (87%) of 2,5-bis[(4′-(*n*-(pentamethyldisiloxyl)butoxy)benzoyl)oxy]toluene as a tan solid. The ^{1}H NMR spectra of the 2,5-bis[(4′-(*n*-(oligodimethylsiloxyl)butoxy)benzoyl)oxy]toluenes with $m = 1, 2$ are identical: 0.08 (s, SiCH_3, $12m + 18$ H), 0.60 (t, CH_2Si, 4 H), 1.53 (m, CH_2CH$_2$Si, 4 H), 1.85 (m, CH_2CH$_2$O, 4 H), 2.26 (s, ArCH_3), 4.06 (t, OCH_2, 4 H), 6.98 (dd, 4 aromatic H ortho to OCH$_2$), 7.14 (m, 3 aromatic H of central ring), 8.16 (dd, 4 aromatic H ortho to CO$_2$Ar). Anal. (C$_{39}$H$_{60}$O$_8$Si$_4$) C, H: calcd, 60.90, 7.86; found, 58.22, 7.80. Anal. (C$_{43}$H$_{72}$O$_{10}$Si$_6$) C, H: calcd, 56.29, 7.91; found, 56.00, 7.94.

The ^{1}H NMR spectra of the 2,5-bis[(4′-(*n*-(oligodimethylsiloxyl)pentoxy)benzoyl)oxy]toluenes with $m = 1, 2$ are identical: 0.08 (s, SiCH_3, $12m + 18$ H), 0.58 (t, CH_2Si, 4 H), 1.42 (m, CH_2CH$_2$Si, 4 H), 1.52 (m, CH_2CH$_2$CH$_2$O, 4 H), 1.84 (m, CH_2CH$_2$O, 4 H), 2.24 (s, ArCH_3), 4.05 (t, OCH_2, 4 H), 6.98 (dd, 4 aromatic H ortho to OCH$_2$), 7.13 (m, 3 aromatic H of central ring), 8.15 (dd, 4 aromatic H ortho to CO$_2$Ar). Anal. (C$_{41}$H$_{64}$O$_8$Si$_4$) C, H: calcd, 57.16, 8.09; found, 55.45, 8.04. Anal. (C$_{45}$H$_{76}$O$_{10}$Si$_6$) C, H: calcd, 57.16, 8.10; found, 55.71, 8.08.

The ^{1}H NMR spectra of the 2,5-bis[(4′-(*n*-(oligodimethylsiloxyl)alkoxy)benzoyl)oxy]toluenes with $n = 6, 8$ and $m = 1, 2$ are identical: 0.08 (s, SiCH_3, $12m + 18$ H), 0.54 (t, CH_2Si, 4 H), 1.37 (m, [CH_2]$_{n-4}$, 4[$n - 4$] H), 1.48 (m, CH_2CH$_2$CH$_2$O, 4 H), 1.83 (m, CH_2CH$_2$O, 4 H), 2.25 (s, ArCH_3), 4.05 (t, OCH_2, 4 H), 6.98 (dd, 4 aromatic H ortho to OCH$_2$), 7.14 (m, 3 aromatic H of central ring), 8.15 (dd, 4 aromatic H ortho to CO$_2$Ar). Anal. (C$_{43}$H$_{68}$O$_8$Si$_4$) C, H: calcd, 62.58, 8.30; found, 61.40, 8.32. Anal. (C$_{47}$H$_{80}$O$_{10}$Si$_6$) C, H: calcd, 57.98, 8.28; found, 56.64, 8.28. Anal. (C$_{47}$H$_{76}$O$_8$Si$_4$) C, H: calcd, 64.04, 8.69; found, 63.79, 8.66. Anal. (C$_{51}$H$_{88}$O$_{10}$Si$_6$) C, H: calcd, 59.49, 8.61; found, 57.76, 8.60.

2,5-Bis[(4′-(*n*-(oligodimethylsiloxyl)alkoxy)benzoyl)-oxy]benzaldehydes ($n = 4$–$6, 8$; $m = 1, 2$). The 2,5-bis[(4′-(*n*-(oligodimethylsiloxyl)alkoxy)benzoyl)oxy]benzaldehydes were synthesized in 35–78% yield as in the following example. A solution of 4′-(*n*-(pentamethyldisiloxyl)butoxy)benzoic acid (1.1 g, 3.3 mmol), 2,5-dihydroxybenzaldehyde (0.22 g, 1.6 mmol), DMAP (0.40 g, 3.3 mmol), *p*-toluenesulfonic acid (63 mg, 0.32 mmol), and DCC (0.76 g, 3.7 mmol) in dry CH$_2$Cl$_2$ (12 mL) was stirred at room temperature for 36 h. The conversion was monitored by TLC, and additional DCC (0.10 g, 0.48 mmol) was added to drive the reaction to completion. Hexanes (70 mL) were added to precipitate dicyclohexylurea, which was filtered off. The filtrate was concentrated using a rotary evaporator, and the resulting viscous oil was purified by column chromatography using silica gel as the stationary phase and a gradient of hexanes/CH$_2$Cl$_2$ (0–70% CH$_2$Cl$_2$) as the eluant to yield 0.46 g (37%) of 2,5-bis[(4′-(*n*-(pentamethyldisiloxyl)butoxy)benzoyl)oxy]benzaldehyde as a gummy liquid. The ^{1}H NMR spectra of the 2,5-bis[(4′-(*n*-(oligodimethylsiloxyl)butoxy)benzoyl)oxy]benzaldehydes with $m = 1, 2$ are identical: 0.08 (s, SiCH_3, $12m + 18$ H), 0.58 (t, CH_2Si, 4 H), 1.48 (m, CH_2CH$_2$Si, 4 H), 1.85 (m, CH_2CH$_2$O, 4 H), 4.06 (t, OCH_2, 4 H), 7.00 (dd, 4 aromatic H ortho to OCH$_2$), 7.39 (d, 1 aromatic H meta to CHO), 7.55 (dd, 1 aromatic H para to CHO), 7.79 (d, 1 aromatic H ortho to CHO), 8.16 (dd, 4 aromatic H ortho to CO$_2$Ar), 10.18 (s, CHO).

The ^{1}H NMR spectra of the 2,5-bis[(4′-(*n*-(oligodimethylsiloxyl)pentoxy)benzoyl)oxy]benzaldehydes with $m = 1, 2$ are

identical: 0.04 (s, SiCH_3, $12m + 18$ H), 0.53 (t, CH_2Si, 4 H), 1.38 (m, CH_2CH$_2$Si, 4 H), 1.50 (m, CH_2CH$_2$CH$_2$O, 4 H), 1.80 (m, CH_2CH$_2$O, 4 H), 4.02 (t, OCH_2, 4 H), 6.95 (dd, 4 aromatic H ortho to OCH$_2$), 8.12 (dd, 4 aromatic H ortho to CO$_2$Ar), 10.16 (s, CHO).

The ^{1}H NMR spectra of the 2,5-bis[(4′-(*n*-(oligodimethylsiloxyl)alkoxy)benzoyl)oxy]benzaldehydes with $n = 6, 8$ and $m = 1, 2$ are identical: 0.07 (s, SiCH_3, $12m + 18$ H), 0.51 (t, CH_2Si, 4 H), 1.33 (m, [CH_2]$_{n-4}$, 4[n-4] H), 1.47 (m, CH_2CH$_2$CH$_2$O, 4 H), 1.83 (m, CH_2CH$_2$O, 4 H), 4.06 (t, OCH_2, 4 H), 6.99 (dd, 4 aromatic H ortho to OCH$_2$), 7.39 (d, 1 aromatic H meta to CHO), 7.53 (dd, 1 aromatic H para to CHO), 7.79 (d, 1 aromatic H ortho to CHO), 8.16 (dd, 4 aromatic H ortho to CO$_2$Ar), 10.20 (s, CHO).

2,5-Bis[(4′-(*n*-(oligodimethylsiloxyl)alkoxy)benzoyl)-oxy]benzyl Alcohols ($n = 4$–$6, 8$; $m = 1, 2$). The 2,5-bis-[(4′-(*n*-(oligodimethylsiloxyl)alkoxy)benzoyl)oxy]benzyl alcohols were synthesized in 56–99% yield as in the following example. Sodium borohydride (50 mg, 1.3 mmol) was added slowly over 1 h to a solution of 2,5-bis[(4′-(*n*-(pentamethyldisiloxyl)butoxy)-benzoyl)oxy]benzaldehyde (0.46 g, 0.58 mmol) in glacial acetic acid (4 mL, 70 mmol) and THF (2 mL) at room temperature. After the reduction was complete according to TLC (50 min), the reaction mixture was poured into cold water (40 mL), and the product was extracted with petroleum ether (40 mL total). The organic extracts were washed with water (30 mL) and then dried over anhydrous MgSO$_4$. After filtration, the solvent was removed in vacuo to yield 0.40 g (87%) of 2,5-bis[(4′-(*n*-(pentamethyldisiloxyl)butoxy)benzoyl)oxy]benzyl alcohol as a white solid. The benzyl alcohols were esterified without purification by recrystallization in order to prevent transesterification. The ^{1}H NMR spectra of the 2,5-bis[(4′-(*n*-(oligodimethylsiloxyl)butoxy)benzoyl)oxy]benzyl alcohols with $m = 1, 2$ are identical: 0.08 (s, SiCH_3, $12m + 18$ H), 0.61 (t, CH_2Si, 4 H), 1.55 (m, CH_2CH$_2$Si, 4 H), 1.86 (m, CH_2CH$_2$O, 4 H), 2.08 (br s, CH$_2$OH), 4.06 (t, OCH_2, 4 H), 4.65 (s, CH_2OH), 6.98 (dd, 4 aromatic H ortho to OCH$_2$), 7.22 (s, 2 aromatic H meta and para to CH$_2$OH), 7.42 (s, 1 aromatic H ortho to CH$_2$OH), 8.14 (dd, 4 aromatic H ortho to CO$_2$Ar).

The ^{1}H NMR spectra of the 2,5-bis[(4′-(*n*-(oligodimethylsiloxyl)pentoxy)benzoyl)oxy]benzaldehydes with $m = 1, 2$ are identical: 0.08 (s, SiCH_3, $12m + 18$ H), 0.57 (t, CH_2Si, 4 H), 1.42 (m, CH_2CH$_2$Si, 4 H), 1.50 (m, CH_2CH$_2$CH$_2$O, 4 H), 1.84 (m, CH_2CH$_2$O, 4 H), 2.08 (br s, CH$_2$OH), 4.05 (t, OCH_2, 4 H), 4.64 (s, CH_2OH), 6.98 (dd, 4 aromatic H ortho to OCH$_2$), 7.21 (s, 2 aromatic H meta and para to CH$_2$OH), 7.41 (s, 1 aromatic H ortho to CH$_2$OH), 8.14 (dd, 4 aromatic H ortho to CO$_2$Ar).

The ^{1}H NMR spectra of the 2,5-bis[(4′-(*n*-(oligodimethylsiloxyl)alkoxy)benzoyl)oxy]benzaldehydes with $n = 6, 8$ and $m = 1, 2$ are identical: 0.08 (s, SiCH_3, $12m + 18$ H), 0.54 (t, CH_2Si, 4 H), 1.37 (m, [CH_2]$_{n-4}$, 4[$n - 4$] H), 1.48 (m, CH_2CH$_2$-CH$_2$O, 4 H), 1.83 (m, CH_2CH$_2$O, 4 H), 2.06 (br s, CH$_2$OH), 4.05 (t, OCH_2, 4 H), 4.64 (s, CH_2OH), 6.98 (dd, 4 aromatic H ortho to OCH$_2$), 7.22 (s, 2 aromatic H meta and para to CH$_2$OH), 7.41 (s, 1 aromatic H ortho to CH$_2$OH), 8.14 (dd, 4 aromatic H ortho to CO$_2$Ar).

5-{[[2′,5′-Bis[(4″-(*n*-(oligodimethylsiloxyl)alkoxy)-benzoyl)oxy]benzyl]oxy]carbonyl}bicyclo[2.2.1]hept-2-ene ($n = 4$–$6, 8$; $m = 1, 2$; 49–73% Endo). The norbornene monomers were prepared in 15–94% yield as in the following example. A solution of bicyclo[2.2.1]hept-2-ene-5-carboxyl chloride (0.14 g, 0.93 mmol) in THF (3 mL) and a solution of triethylamine (95 mg, 0.94 mmol) in THF (3 mL) were simultaneously added dropwise over 50 min to an ice-cooled solution of 2,5-bis[(4′-(*n*-(pentamethyldisiloxyl)butoxy)benzoyl)-oxy]benzyl alcohol (0.52 g, 0.66 mmol) in THF (4 mL). The reaction mixture was slowly warmed to room temperature and was stirred for a total of 26 h. The precipitated triethylammonium chloride was filtered off, and the filtrate was concentrated in vacuo. The residue was purified by column chromatography using silica gel as the stationary phase and a gradient of hexanes/CH$_2$Cl$_2$ as the eluant, followed by two reprecipitations from CH$_2$Cl$_2$ (1 mL) into cold (−78 °C) methanol (10 mL) to yield 0.25 g (41%) of 5-{[[2′,5′-bis[(4″-(*n*-(pentamethyldisiloxyl)butoxy)benzoyl)oxy]benzyl]oxy]carbonyl}-

bicyclo[2.2.1]hept-2-ene as a colorless gummy solid. The monomer was purified for polymerization by azeotropic distillation of water with hexanes in the drybox, followed by drying in vacuo. The ^{1}H NMR spectra of the 5-{[[2′,5′-bis[(4″-(*n*-(oligodimethylsiloxyl)butoxy)benzoyl)oxy]benzyl]oxy]carbonyl}-bicyclo[2.2.1]hept-2-enes with $m = 1, 2$ are identical: resonances at 1.24 (d), 2.19 (s), 2.87 (m), 2.97 (m), and 3.14 (s) are due to the nonolefinic norbornene protons of both isomers; 0.06 (s, SiCH_3, 12m + 18 H), 0.60 (t, CH_2Si, 4 H), 1.55 (m, CH_2-CH$_2$Si, 4 H), 1.85 (m, CH_2CH$_2$O, 4 H), 4.06 (t, OCH_2, 4 H), 5.08 (d, CH_2Ar, endo), 5.14 (s, CH_2Ar, exo), 5.80 (m, 1 olefinic H, endo), 6.07 (m, 1 olefinic H, exo), 6.10 (m, 1 olefinic H of both isomers), 6.98 (dd, 4 aromatic H ortho to OCH$_2$), 7.29 (m, 3 aromatic H of central ring), 8.14 (dd, 4 aromatic H ortho to CO$_2$Ar). Anal. (C$_{47}$H$_{68}$O$_{10}$Si$_4$, 54% endo) C, H: calcd, 62.34, 7.57; found, 62.48, 7.64. Anal. (C$_{51}$H$_{80}$O$_{12}$Si$_6$, 51% endo) C, H: calcd, 58.13, 7.65; found, 57.97, 7.56.

The ^{1}H NMR spectra of the 5-{[[2′,5′-bis[(4″-(*n*-(oligo-dimethylsiloxyl)pentoxy)benzoyl)oxy]benzyl]oxy]carbonyl}bicyclo-[2.2.1]hept-2-enes with $m = 1, 2$ are identical: resonances at 1.23 (d), 2.18 (s), 2.86 (m), 2.94 (m), and 3.14 (s) are due to the nonolefinic norbornene protons of both isomers; 0.06 (s, SiCH_3, 12m + 18 H), 0.56 (t, CH_2Si, 4 H), 1.44 (m, [CH_2]$_2$, 8 H), 1.84 (m, CH_2CH$_2$O, 4 H), 4.05 (t, OCH_2, 4 H), 5.08 (d, CH_2-Ar, endo), 5.14 (s, CH_2Ar, exo), 5.80 (m, 1 olefinic H, endo), 6.05 (m, 1 olefinic H, exo), 6.10 (m, 1 olefinic H of both isomers), 6.98 (dd, 4 aromatic H ortho to OCH$_2$), 7.28 (m, 3 aromatic H of central ring), 8.14 (dd, 4 aromatic H ortho to CO$_2$Ar). Anal. (C$_{49}$H$_{72}$O$_{10}$Si$_4$, 72% endo) C, H: calcd, 63.05, 7.77; found, 64.07, 7.75. Anal. (C$_{53}$H$_{84}$O$_{12}$Si$_6$, 52% endo) C, H: calcd, 58.85, 7.83; found, 58.50, 7.81.

The ^{1}H NMR spectra of the 5-{[[2′,5′-bis[(4″-(*n*-(oligo-dimethylsiloxyl)alkoxy)benzoyl)oxy]benzyl]oxy]carbonyl}bicyclo-[2.2.1]hept-2-enes with $n = 6, 8$ and $m = 1, 2$ are identical: resonances at 1.23 (d), 2.20 (s), 2.85 (m), 2.96 (m) and 3.14 (s) are due to the nonolefinic norbornene protons of both isomers; 0.08 (s, SiCH_3, 12m + 18 H), 0.54 (t, CH_2Si, 4 H), 1.37 (m, [CH_2]$_{n-4}$, 4[n − 4] H), 1.48 (m, CH_2CH$_2$CH$_2$O, 4 H), 1.83 (m, CH_2CH$_2$O, 4 H), 4.06 (t, OCH_2, 4 H), 5.08 (d, CH_2Ar, endo), 5.14 (s, CH_2Ar, exo), 5.80 (m, 1 olefinic H, exo), 6.07 (m, 1 olefinic H, exo), 6.10 (m, 1 olefinic H of both isomers), 6.98 (dd, 4 aromatic H ortho to OCH$_2$), 7.26 (m, 3 aromatic H of central ring), 8.14 (dd, 4 aromatic H ortho to CO$_2$Ar). Anal. (C$_{51}$H$_{76}$O$_{10}$Si$_4$, 49% endo) C, H: calcd, 63.70, 7.97; found, 63.98, 7.92. Anal. (C$_{55}$H$_{88}$O$_{12}$Si$_6$, 55% endo) C, H: calcd, 59.52, 7.99; found, 59.20, 7.96. Anal. (C$_{55}$H$_{84}$O$_{10}$Si$_4$, 63% endo) C, H: calcd, 64.92, 8.32; found, 64.42, 8.53. Anal. (C$_{59}$H$_{96}$O$_{12}$Si$_6$, 80% endo) C, H: calcd, 60.78, 8.30; found, 60.50, 8.26.

Poly{5-[[[2′,5′-bis[(4″-(*n*-(oligodimethylsiloxyl)alkoxy)-benzoyl)oxy]benzyl]oxy]carbonyl]bicyclo[2.2.1]hept-2-ene}s ($n = 4$−6, 8; $m = 1, 2$). The polymers were prepared in 82−98% yield. In a typical procedure, a solution of 5-{[[2′,5′-bis[(4″-(*n*-(pentamethyldisiloxyl)butoxy)benzoyl)oxy]-benzyl]oxy]carbonyl}bicyclo[2.2.1]hept-2-ene (0.20 g, 0.22 mmol) in dry THF (2.5 g) was added dropwise over 2 min to a solution of Mo(CHCMe$_2$Ph)(N-2,6-^{i}Pr$_2$Ph)(O^{t}Bu)$_2$ (2.5 mg, 4.5 μmol) in dry THF (1.0 g). After stirring at room temperature for 2 h, the orange solution was quenched with benzaldehyde and then stirred for 30 min. The solution was taken outside of the drybox and precipitated in methanol (90 mL). The precipitate was collected, dried, and reprecipitated from CH$_2$Cl$_2$ (150 mL) into methanol (125 mL) to yield 0.16 g (82%) of poly{5-[[[2′,5′-bis[(4″-(*n*-(pentamethyldisiloxyl)butoxy)benzoyl)oxy]benzyl]-oxy]carbonyl]bicyclo[2.2.1]hept-2-ene} as a white powder: M_n = 4.69 × 10^4, pdi = 1.57.

Supporting Information Available: Differential scanning calorimetry traces of the 2,5-bis[(4′-(*n*-(oligodimethylsiloxyl)alkoxy)benzoyl)oxy]toluene model compounds ($n = 4$−6, 8; $m = 1, 2$) observed on heating and on cooling at 10 °C/min (1 page). Ordering information is given on any current masthead page.

References and Notes

(1) Arehart, S. V.; Pugh, C. *J. Am. Chem. Soc.* **1997**, *119*, 3027.
(2) (a) Pugh, C.; Arehart, S.; Liu, H.; Narayanan, R. *J. Macromol. Sci.—Pure Appl. Chem.* **1994**, *A31*, 1591. (b) Pugh, C.; Liu, H.; Arehart, S.; Narayanan, R. *Macromol. Symp.* **1995**, *98*, 293.
(3) Scott, R. L. *J. Phys. Chem.* **1958**, *62*, 136.
(4) Dunlap, R. D.; Bedford, R. G.; Woodbrey, J. C.; Furrow, S. D. *J. Am. Chem. Soc.* **1959**, *81*, 2927.
(5) Bedford, R. G.; Dunlap, R. D. *J. Am. Chem. Soc.* **1958**, *80*, 282 and references therein.
(6) Höpken, J. Ph.D. Thesis, Universiteit Twente, 1991.
(7) (a) Hildebrand, J. H.; Fisher, B. B.; Benesi, H. A. *J. Am. Chem. Soc.* **1950**, *72*, 4348. (b) Young, C. L. *Trans. Faraday Soc.* **1969**, 2639 and references therein.
(8) Dorset, D. L. *Macromolecules* **1990**, *23*, 894.
(9) (a) Koden, M.; Nakagawa, K.; Ishii, Y.; Funada, F.; Matsuura, M.; Awane, A. *Mol. Cryst. Liq. Cryst. Lett.* **1989**, *6*, 185. (b) Doi, T.; Sakurai, Y.; Tamatani, A.; Takenaka, S.; Kusabayashi, S.; Nishihata, Y.; Terauchi, H. *J. Mater. Chem.* **1991**, *1*, 169. (c) Volkov, V. V.; Platé, N. A.; Takahara, A.; Kajiyama, T.; Amaya, N.; Murata, Y. *Polymer* **1992**, *33*, 1316. (d) Wilson, L. M.; Griffin, A. C. *Macromolecules* **1993**, *26*, 6312. (e) Lobko, T. A.; Ostrovskii, B. J.; Pavluchenko, A. I.; Sulianov, S. N. *Liq. Cryst.* **1993**, *15*, 361. (f) Wilson, L. M.; Griffin, A. C. *Macromolecules* **1994**, *27*, 1928. (g) Wilson, L. M.; Griffin, A. C. *Macromolecules* **1994**, *27*, 4611. (h) Wilson, L. M. *Liq. Cryst.* **1994**, *17*, 277. (i) Wilson, L. M. *Macromolecules* **1995**, *28*, 325. (j) Davidson, T.; Griffin, A. C.; Wilson, L. M.; Windle, A. H. *Macromolecules* **1995**, *28*, 354. (k) Cumming, W. J.; Gaudiana, R. A. *Liq. Cryst.* **1996**, *20*, 283. (l) Liu, H.; Nohira, H. *Liq. Cryst.* **1997**, *22*, 217.
(10) Elias, H. G. *Macromolecules. Structure and Properties*, 2nd ed.; Plenum: New York, 1984; pp 98−103.
(11) (a) Guillon, D.; Skoulios, A. *J. Phys.* **1976**, *45*, 607. (b) Ringsdorf, H.; Schlarb, B.; Venzmer, J. *Angew. Chem., Int. Ed. Engl.* **1988**, *27*, 113.
(12) Bunn, C.; Howells, E. R. *Nature* **1954**, *174*, 549.
(13) Clark, E. S.; Muus, L. T. *Z. Kristallogr.* **1962**, *117*, 119.
(14) Pieszek, W.; Strobl, G. R.; Malzahn, K. *Acta Crystallogr.* **1974**, *B30*, 1278.
(15) Schwickert, H.; Strobl, G.; Kimmig, M. *J. Chem. Phys.* **1991**, *95*, 2800: from unit cell of perfluoro-*n*-eicosane, $a = b = 5.70$ Å.
(16) *Polymer Handbook*, 3rd ed.; Brandrup, J., Immergut, E. H., Eds.; Wiley-Interscience: New York, 1989.
(17) Nishioka, A.; Watanabe, M. *J. Polym. Sci.* **1957**, *24*, 298.
(18) $C_\infty = \langle R^2 \rangle / n l^2$, where $\langle R^2 \rangle$ is the mean-square end-to-end distance of the chains, n is the number, and l^2 is the root-mean-square average length of backbone bonds for large n.
(19) Matsuo, K.; Stockmayer, W. H. *J. Phys. Chem.* **1981**, *85*, 3307.
(20) Chu, B.; Wu, C.; Buck, W. *Macromolecules* **1989**, *22*, 831.
(21) Bates, T. W.; Stockmayer, W. H. *Macromolecules* **1968**, *1*, 17.
(22) Chiang, R. *J. Phys. Chem.* **1965**, *69*, 1645.
(23) Smith, G. D.; Jaffe, R. L.; Yoon, D. Y. *Macromolecules* **1994**, *27*, 3166.
(24) (a) Crescenzi, V.; Flory, P. J.; Mark, J. E. *J. Am. Chem. Soc.* **1964**, *86*, 141. (b) Flory, P. J.; Semlyen, J. A. *J. Am. Chem. Soc.* **1966**, *88*, 3209.
(25) Stepto, R. F. T. In *Siloxane Polymers*; Clarson, S. J., Semleyen, J. A., Eds.; PTR Prentice Hall: Englewood Cliffs, NJ, 1993; Chapter 8.
(26) Flory, P. J.; Crescenzi, V.; Mark, J. E. *J. Am. Chem. Soc.* **1964**, *86*, 146.
(27) Flory, P. J. *Statistical Mechanics of Chain Molecules*; Hanser: Munich, 1989; Chapter V.10.
(28) Damaschun, G. *Kolloid Z.* **1962**, *180*, 65.
(29) Boyer, R. F.; Miller, R. L. *Rubber Chem. Technol.* **1978**, *51*, 718.
(30) (a) Coles, H. J.; Owen, H.; Newton, J.; Hodge, P. *Liq. Cryst.* **1993**, *15*, 739. (b) Naciri, J.; Ruth, J.; Crawford, G.; Shash-

idhar, R.; Ratna, B. R. *Chem. Mater*. **1995**, *7*, 1397. (c) Ibn-Elhaj, M.; Skoulios, A.; Guillon, D.; Newton, J.; Hodge, P. Coles. H. J. *J. Phys. II Fr.* **1996**, *6*, 271.

(31) (a) Braun, F.; Willner, L.; Hess, M.; Kosfeld, R. *Markomol. Chem., Rapid Commun.* **1989**, *10*, 51. (b) Sunohara, K.; Takatoh, K.; Sakamoto, M. *Liq. Cryst.* **1993**, *13*, 283. (c) Ibn-Elhaj, M.; Coles, H. J.; Guillon, D.; Skoulios, A. *J. Phys. II Fr.* **1993**, *3*, 1807. (d) Newton, J.; Coles, H.; Hodge, P.; Hannington, J. *J. Mater. Chem.* **1994**, *4*, 869. (e) Vieth, C. A.; Samulski, E. T.; Murthy, N. S. *Liq. Cryst.* **1995**, *19*, 557.

(32) (a) Loos-Wildenauer, M.; Kunz, S.; Voigt-Martin, I. G.; Yakimanski, A.; Wischerhoff, E.; Zentel, R.; Tschierske, C.; Müller, M. *Adv. Mater.* **1995**, *7*, 170.

(33) (a) Aquilera, C.; Bernal, L. *Polym. Bull.* **1984**, *12*, 383. (b) Hardouin, F.; Richard, H.; Achard, M. F. *Liq. Cryst.* **1993**, *14*, 971. (c) Ibn-Elhaj, M.; Skoulios, A.; Guillon, D.; Newton, J.; Hodge, P.; Cole, H. J. *Liq. Cryst.* **1995**, *19*, 373.

(34) (a) Creed, D.; Gross, J. R. D.; Sullivan, S. L.; Griffin, A. C.; Hoyle, C. E. *Mol. Cryst. Liq. Cryst.* **1987**, *149*, 185. (b) Hohmuth, A.; Schiewe, B.; Heinemann, S.; Kresse, H. *Liq. Cryst.* **1997**, *22*, 211.

(35) (a) Keller, P.; Shao, R.; Walba, D. M.; Brunet, M. *Liq. Cryst.* **1995**, *18*, 915.

(36) (a) Aguilera, C.; Bartulin, J.; Hisgen, B.; Ringsdorf, H. *Makromol. Chem.* **1983**, *184*, 253. (b) Ozcayir, Y.; Lai, X.; Ratto, J.; Blumstein, A. *Mol. Cryst. Liq. Cryst.* **1990**, *185*, 75. (c) Diaz, F.; Tagle, L. H.; Valdebenito, N.; Aguilera, C. *Polymer* **1993**, *34*, 418.

(37) (a) Jo, B.-W.; Jin, J. I.; Lenz, R. W. *Eur. Polym. J.* **1982**, *18*, 233. (b) Creed, D.; Griffin, A. C.; Gross, J. R. D.; Hoyle, C. E.; Venkataram, K. *Mol. Cryst. Liq. Cryst.* **1988**, *155*, 57. (c) Zuev, V. V.; Smirnova, G. S.; Nikonorova, N. A.; Borisova, T. I.; Skorokhodov, S. S. *Makromol. Chem.* **1990**, *191*, 2865.

(38) (a) Engel, M.; Hisgen, B.; Keller, R.; Kreuder, W.; Reck, B.; Ringsdorf, H.; Schmidt, H.-W.; Tschirner, P. *Pure Appl. Chem.* **1985**, *57*, 1009. (b) Kawakami, Y.; Toida, K.; Ito, Y. *Macromolecules* **1993**, *26*, 1177. (c) Nagase, Y.; Takamura, Y.; Abe, H.; Ono, K.; Saito, T.; Akiyama, E. *Makromol. Chem.* **1993**, *194*, 2517. (d) Kawakami, Y.; Toida, K. *Macromolecules* **1995**, *28*, 816. (e) Kawakami, Y.; Inoue, H.; Kishimoto, N.; Mori, A. *Polym. Bull.* **1996**, *36*, 653.

(39) (a) Kawakami, Y.; Ichitani, M.; Kunisada, H.; Yuki, Y. *Polym. J.* **1996**, *28*, 513. (b) Kawakami, Y.; Suzuki, M.; Kaito, Y.; Mori, A. *Polym. J.* **1996**, *28*, 845.

(40) (a) Hessel, F.; Finkelmann, H. *Polym. Bull.* **1985**, *14*, 375. (b) Hessel, F.; Herr, R.-P.; Finkelmann, H. *Makromol. Chem.* **1987**, *188*, 1597. (c) Zhou, Q.-F.; Li, H.-M.; Feng, X. D. *Macromolecules* **1987**, *20*, 233. (d) Zhou, Q.-F.; Li, H.-M.; Feng, X. D. *Mol. Cryst. Liq. Cryst.* **1988**, *155*, 73. (e) Keller, P.; Hardouin, F.; Mauzac, M.; Achard, M. F. *Mol. Cryst. Liq. Cryst.* **1988**, *155*, 171. (f) Attard, G. S.; Araki, K.; Moura-Ramos, J. J.; Williams, G. *Liq. Cryst.* **1988**, *3*, 861. (g) Hessel, F.; Finkelmann, H. *Makromol. Chem.* **1988**, *189*, 2275. (h) Hardouin, F.; Mery, S.; Achard, M. F.; Mauzac, M.; Davidson, P.; Keller, P. *Liq. Cryst.* **1990**, *8*, 565. (i) Hardouin, F.; Mery, S.; Achard, M. F.; Noirez, L.; Keller, P. *J. Phys. II Fr.* **1991**, *1*, 511. (j) Hardouin, F.; Leroux, N.; Mery, S.; Noirez, L. *J. Phys. II Fr.* **1992**, *2*, 271. (k) Lewthwaite, R. A.; Gray, G. W.; Toyne, K. J. *J. Mater. Chem.* **1992**, *2*, 119. (l) Percec, V.; Tomazos, D. *J. Mater. Chem.* **1993**, *3*, 643. (m) Leroux, N.; Keller, P.; Achard, M. F.; Noirez, L.; Hardouin, F. *J. Phys. II Fr.* **1993**, *3*, 1289. (n) Cherodian, A. S.; Hughes, N. J.; Richardson, R. M.; Lee, M. S. K.; Gray, G. W. *Liq. Cryst.* **1993**, *14*, 1667. (o) Achard, M. F.; Lecommandoux, S.; Hardouin, F. *Liq. Cryst.* **1995**, *19*, 581. (p) Takenaka, S.; Yamasaki, Y. *Mol. Cryst. Liq. Cryst.* **1995**, *258*, 51. (q) Jego, C.; Leroux, N.; Agricole, B.; Mingotaud, C. *Liq. Cryst.* **1996**, *20*, 691. (r) Leroux, N.; Chien, L.-C. *Liq. Cryst.* **1996**, *21*, 189. (s) Lecommandoux, S.; Achard, M. F.; Hardouin, F.; Brulet, A.; Cotton, J. P. *Liq. Cryst.* **1997**, *22*, 549.

(41) Pugh, C.; Shrock, R. R. *Macromolecules* **1992**, *25*, 6593.

(42) Pugh, C.; Dharia, J.; Arehart, S. V. *Macromolecules* **1997**, *30*, 4520.

(43) Pugh, C.; Kiste, A. L. *Prog. Polym. Sci.* **1997**, *22*, 601.

(44) Christensen, J. J.; Hanks, R. W.; Izatt, R. M. *Handbook of Heats of Mixing*; Wiley: New York, 1982.

(45) (a) Gray, G. W.; Goodby, J. W. *Smectic Liquid Crystals. Textures and Structures*; Leonard Hall: Glasgow, 1984. (b) Demus, D.; Richter, L. *Textures of Liquid Crystals*; Verlag Chemie: Weinheim, 1978.

(46) (a) Schrock, R. R.; Murdzek, J. S.; Bazan, G. C.; Robbins, J.; DiMare, M.; O'Regan, M. *J. Am. Chem. Soc.* **1990**, *112*, 3875. (b) Fox, H. H.; Yap, K. B.; Robbins, J.; Cai, S.; Schrock, R. R. *Inorg. Chem.* **1992**, *31*, 2287.